nature climate change

ARTICLES

https://doi.org/10.1038/s41558-021-01007-8

No projected global drylands expansion under greenhouse warming

Alexis Berg[1]✉ and Kaighin A. McColl[1,2]

Drylands, comprising land regions characterized by water-limited, sparse vegetation, have commonly been projected to expand globally under climate warming. Such projections, however, rely on an atmospheric proxy for drylands, the aridity index, which has recently been shown to yield qualitatively incorrect projections of various components of the terrestrial water cycle. Here, we use an alternative index of drylands, based directly on relevant ecohydrological variables, and compare projections of both indices in Coupled Model Intercomparison Project Phase 5 climate models as well as Dynamic Global Vegetation Models. The aridity index overestimates simulated ecohydrological index changes. This divergence reflects different index sensitivities to hydroclimate change and opposite responses to the physiological effect on vegetation of increasing atmospheric CO_2. Atmospheric aridity is thus not an accurate proxy of the future extent of drylands. Despite greater uncertainties than in atmospheric projections, climate model ecohydrological projections indicate no global drylands expansion under greenhouse warming, contrary to previous claims based on atmospheric aridity.

Global drylands are regions of the world where ecosystems are water-limited, soils are often relatively infertile and vegetation cover is sparse[1,2]. They encompass water-limited ecosystems such as deserts, grasslands, shrublands and savanna woodlands and currently cover around 40% of the land surface[1]. They also host nearly 40% of the global population[3], supporting the livelihood of large rural populations. As climate warms, potential increases in the aridity of existing drylands and in their spatial extent may thus have profound adverse human and socio-economic impacts. In addition to their importance for the human population and economy, recent research has shown the critical global ecological role played by drylands[4].

To study drylands, a quantitative definition of these regions is needed. Regions conventionally defined as drylands span a range of land environments sharing some similar climatological and ecological characteristics: dry climate, water limitation and scarce vegetation. As such, there is no single atmospheric or land surface variable that can be used to quantitatively identify these regions—instead, a multivariate index must be employed. The most common definition is based on the aridity index (AI)—that is, the ratio of mean annual precipitation (P) to potential evapotranspiration (PET, representing the evaporative demand of the air near the surface; Methods). Under the Middleton and Thomas[5] scheme, adopted by the United Nations, drylands are regions where $AI < 0.65$. This definition is based on the long-standing observation that similar AI values correspond to broadly similar vegetation types around the world, with lower values corresponding to drier ecosystems, as evaporative demand exceeds precipitation[6]. This definition also only requires atmospheric observations, which have historically been easier to obtain than hydrological or ecosystem measurements.

Building on that definition, an expanding body of literature based on the AI calculated from climate model output suggests that as climate warms, drylands will expand globally, perhaps dramatically, as continental PET increases faster than P[7–16]. Such projections are often used to inform ecological impact assessments of future climate change[17].

However, the rationale for using the AI in climate projections to assess future drylands dynamics is debatable. First, land surface data limitations are no longer a concern when using climate model outputs rather than real-world observations. More physically meaningful measures of aridity are directly available from climate model land surface outputs, such as soil moisture or vegetation, eliminating the need for offline indices such as the AI. Second, the AI, as an atmosphere-based metric, is only a proxy for the actual land characteristics associated with drylands, such as limited water availability and low vegetation density. A crucial but seldom evaluated assumption in AI-based studies is that this proxy relationship, established over present-day climate[5], is stationary under climate change[17,18]. However, recent research has demonstrated problems with this assumption, showing the AI to be a negatively biased (that is, too arid) estimator of model-simulated future changes in various land surface variables, such as global water cycle and carbon cycle changes[19,20]. A salient issue is that common calculations of Penman–Monteith PET used in future AI estimates probably overestimate the future evaporative demand, in part by neglecting changes in vegetation physiology under higher CO_2 (refs. [21,22]), thus leading to excessively arid future AI values (all other things being equal). Additionally, the approach does not account for environmental effects that may alter the relationship between climate and land characteristics, such as the CO_2 fertilization effect[23].

Although these problems with the AI will probably affect future drylands assessments[20], the potential implications for projections of drylands expansion are unknown. Here, we address this critical gap by revisiting projections of future drylands using analyses that are independent of the AI. Using Coupled Model Intercomparison Project Phase 5 (CMIP5) models, we derive an alternative index of drylands, the ecohydrological index (EI), directly based on land surface ecohydrological properties. We compare drylands projections in climate change projections using both the AI and the EI. Furthermore, we analyse the causes of the differential responses of both metrics (AI and EI) to greenhouse warming, focusing in

[1]Department of Earth and Planetary Sciences, Harvard University, Cambridge, MA, USA. [2]School of Engineering and Applied Sciences, Harvard University, Cambridge, MA, USA. ✉e-mail: alexis_berg@fas.harvard.edu

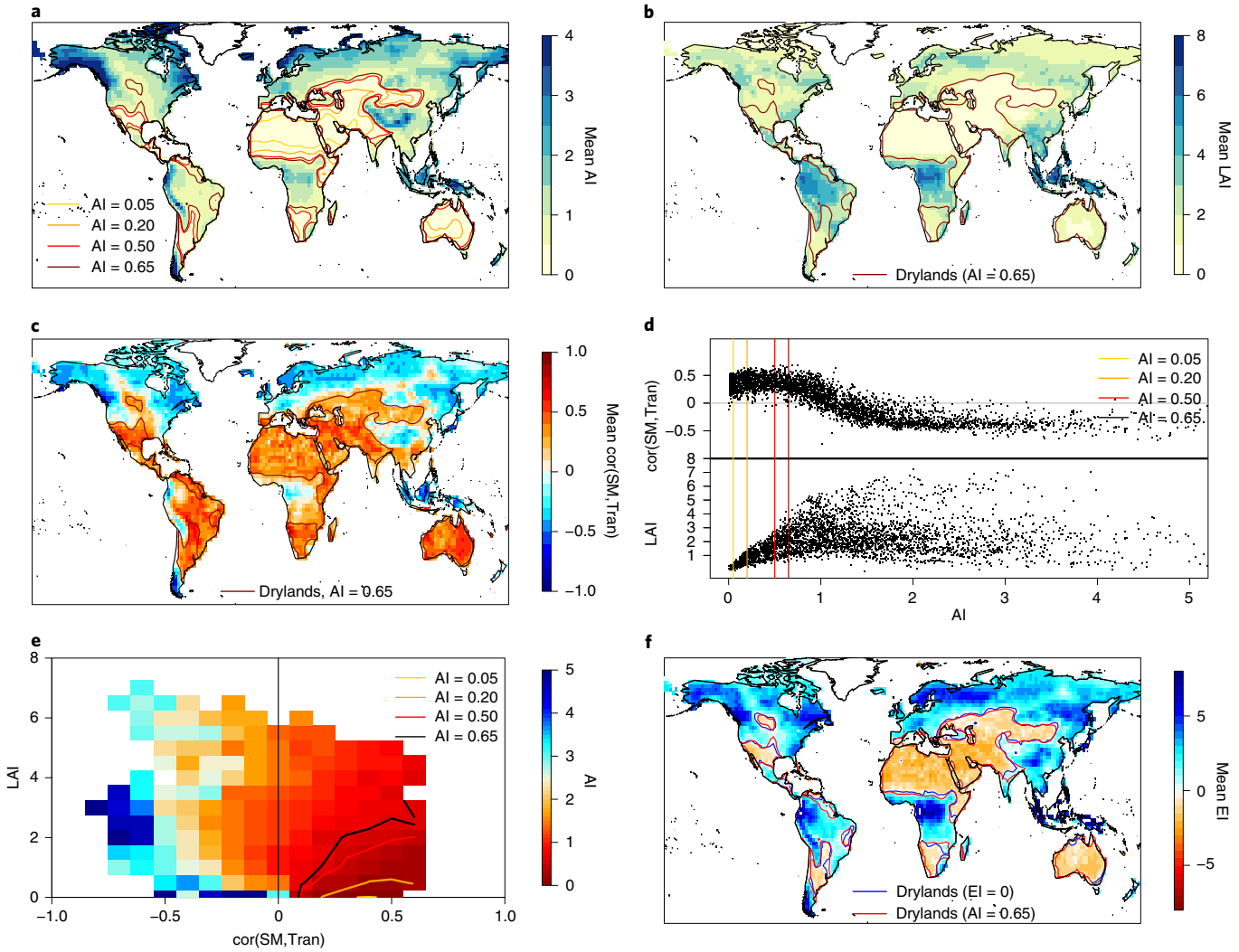

Fig. 1 | Establishing an EI of drylands in CMIP5 models. a, Multimodel mean AI in 12 CMIP5 models (Methods and Supplementary Table 1) and corresponding drylands classification[5] over 1971–2000: hyperarid (AI < 0.05), arid (0.05 < AI < 0.2), semi-arid (0.2 < AI < 0.5) and dry subhumid (0.5 < AI < 0.65). **b**, Multimodel mean annual LAI; the contour lines represent drylands according to the AI-based definition (AI < 0.65). **c**, Multimodel mean cor(SM,Tran); the contour lines are the same as in **b**. **d**, Relationship over global land between the AI and LAI or cor(SM,Tran), from **a**–**c**; the vertical lines correspond to the AI thresholds denoted in **a**. **e**, Multimodel mean AI binned as a function of mean cor(SM,Tran) and mean LAI. **f**, Multimodel mean EI (Methods); the contour lines indicate drylands based on the AI and EI definitions.

particular on the role of vegetation physiological responses under higher atmospheric CO_2.

An EI of drylands

The global pattern of the AI simulated in CMIP5 models for present-day climate includes higher values (less arid) in tropical and high latitudes, and lower (more arid) values in subtropical latitudes[9]. Drylands, as defined on the basis of the AI criteria (AI < 0.65), occupy large parts of the continental subtropics (Fig. 1a).

Definitions of drylands—excluding those based on the AI—focus on the determining role of water availability in controlling ecosystem productivity and other plant processes[1]; this water limitation is also reflected in sparse vegetation[2]. In the same CMIP5 models, we characterize these two defining characteristics by the simulated correlation between annual mean surface soil moisture (Methods) and transpiration (cor(SM,Tran)) and by the leaf area index (LAI), respectively. Positive values of cor(SM,Tran) indicate a soil-moisture-limited transpiration regime; negative values reflect an energy-limited regime[24]. We focus on soil moisture limitation instead of absolute soil water content because soil moisture limitation is more directly relevant to the functional definition of drylands as water-limited ecosystems[1], especially under a changing climate (Discussion and conclusions).

In present-day climate, a broad spatial relationship exists in CMIP5 models between AI-defined drylands and regions exhibiting low simulated vegetation and positive cor(SM,Tran) (Fig. 1b–d). The AI thus spatially overlaps with key ecohydrological aspects of drylands, justifying its use as a proxy for drylands under present-day climate. However, some regions exhibit both high LAI and positive soil moisture limitation (for example, the Amazon and Southeast Asia), while others exhibit low LAI but no moisture limitation (high latitudes). Figure 1e shows that AI-defined drylands can be equated with regions with both low vegetation cover and water-limited transpiration, illustrating that both quantities are central to the ecohydrological definition of drylands. On the basis of this finding, we define an EI of drylands as a linear function of LAI and cor(SM,Tran), which is specifically designed to be negative in drylands (Methods). As opposed to the AI, which characterizes

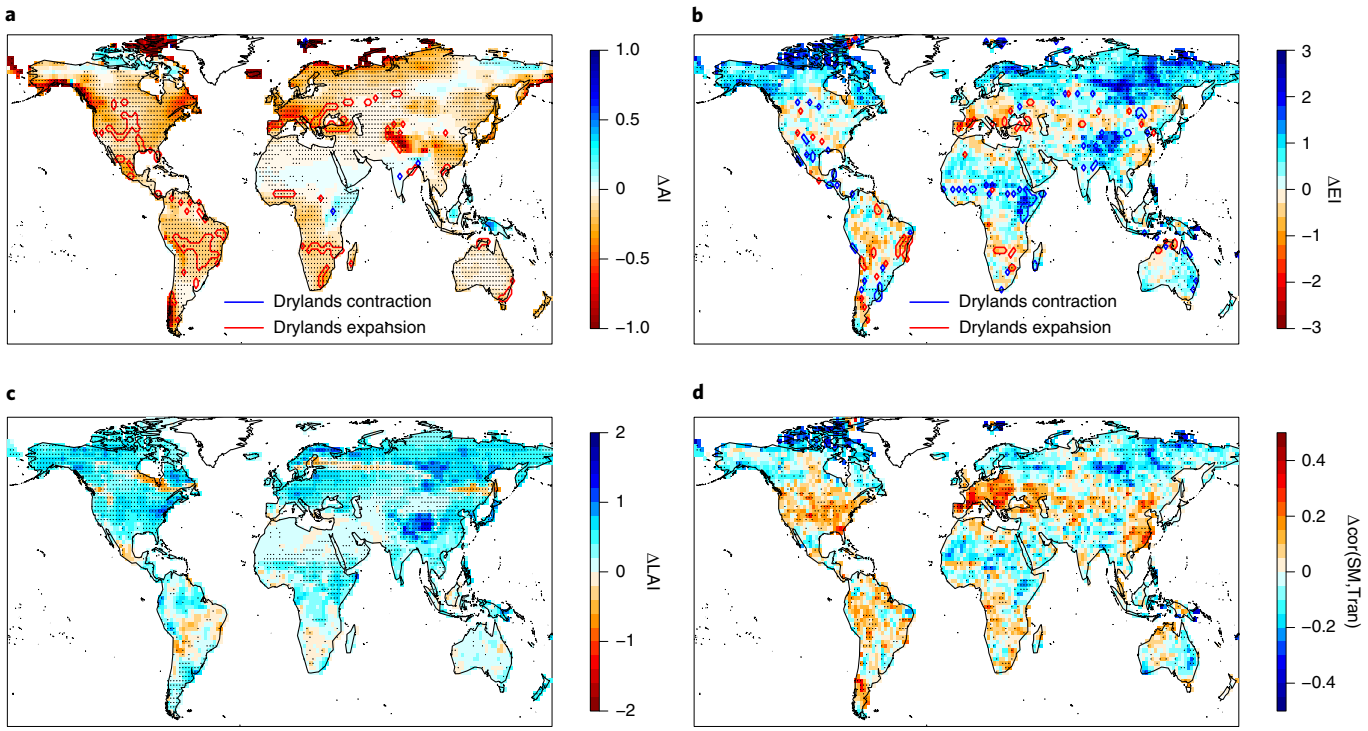

Fig. 2 | Divergent AI and EI projections under climate change in CMIP5 models. a, Mean change in AI between 1971–2000 and 2071–2100 in the RCP8.5 scenario. The contour lines indicate changes in drylands defined on the basis of the AI. **b**, Same as **a**, for the EI. **c**, Mean change in LAI. **d**, Change in cor(SM,Tran). The stippling indicates where more than three-quarters of models agree on the sign of the change.

atmospheric aridity, the EI is an index of ecohydrological aridity: lower EI values correspond to more water-limited vegetation and lower vegetation density. We emphasize that this index is empirically derived from climate models, by matching simulated AI-defined drylands with relevant simulated land surface outputs (Fig. 1e,f). We thus do not seek to justify the exact index formulation with observational or theoretical considerations. Rather, the index is introduced as a tool to test the hypothesis that drylands are truly expanding in climate model projections.

Divergence between AI and EI projections

Under a high-emission scenario (Representative Concentration Pathway 8.5 (RCP8.5)), the projected AI values in climate models decrease over most of the land surface, indicating a global increase in atmospheric aridity[7–16]; consequently, AI-defined drylands expand in most places (Fig. 2a). However, land surface outputs from the same CMIP5 models project more balanced changes in ecohydrological conditions, with the EI decreasing in some regions (that is, trending towards more water-limited and/or sparser vegetation) and increasing in others (that is, trending towards less water-limited and/or denser vegetation) (Fig. 2b). Accordingly, EI-defined drylands expand but also contract in various regions (for example, East Africa). In regions where AI-defined drylands expand, EI changes are often positive (Supplementary Fig. 1).

This EI response emerges from a combination of responses in LAI and soil moisture limitation both less uniformly negative than the AI (Fig. 2c,d). CMIP5 LAI projections show widespread increases[25], except in some limited subtropical regions and in a narrow band at high latitudes, where a few models project LAI decrease, presumably because of the loss of boreal forests under warming. Soil moisture limitation on transpiration exhibits more contrasted patterns, with increased water limitation in Northern Hemisphere midlatitude regions in particular (North America, Europe and eastern China). In parts of these regions, increased water limitation dominates the LAI increase in EI changes, leading to a decrease in the EI; however, most often the LAI increase dominates, leading to positive EI changes. Many regions (for example, high latitudes, East Africa and South Asia) show both LAI increases and decreased water limitation.

The discrepancy between projected atmospheric and ecohydrological indices demonstrates that, while the AI may be a proxy for drylands under the current climate, it does not accurately capture projected changes in the ecohydrological conditions associated with drylands. This discrepancy is further reflected in the non-stationarity of the relationship between the AI and ecohydrological properties: under future climate, AI-defined drylands encompass a broader, less ecohydrologically arid set of LAI and water limitation values than under present climate (Supplementary Fig. 2).

Climatic drivers of the AI–EI divergence

The AI decreases in a warmer climate are primarily driven by a warming-induced increase in PET, which dominates the smaller increase in P over land[8,9,26]. Increased atmospheric aridity can thus occur even when P increases (Fig. 3a); the interpretation is that greater increases in evaporative demand will eventually dry out the land surface by depleting land moisture. However, under such conditions, ecohydrological aridity decreases in CMIP5 models (Fig. 3b); the EI tends to decrease only when P decreases. This response reflects a broadly similar behaviour in both LAI and soil moisture limitation (Supplementary Fig. 3). Soil moisture limitation does increase in some regions with moderate P increases and larger PET increases (Supplementary Fig. 3b); however, vegetation still increases in such regions, indicating that this increased water limitation does not come at the expense of vegetation growth. Figure 3 suggests a dominant role of P changes, rather than PET, in driving changes in ecohydrological conditions in climate models. Furthermore, the joint distribution of ΔPET and ΔP (Supplementary Fig. 3c) also indicates some level of coupling between both quantities: the more

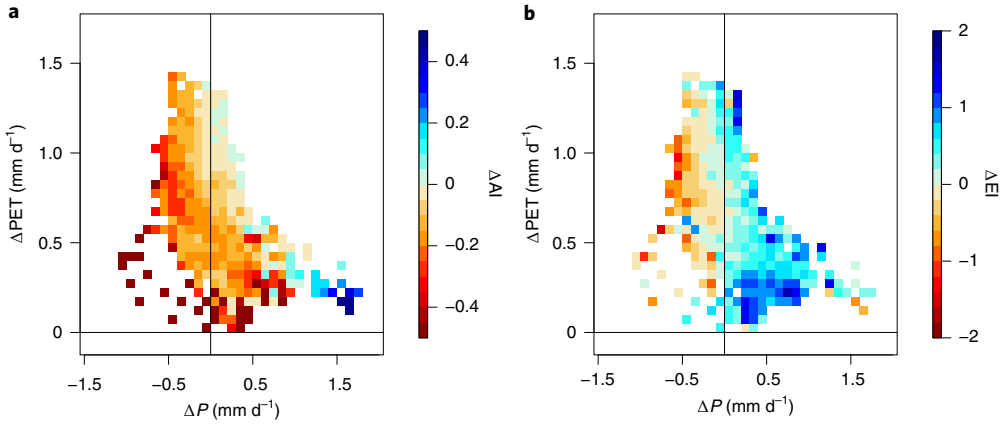

Fig. 3 | Different sensitivities of the EI and the AI to hydroclimatic changes. a, Changes in AI in CMIP5 models in RCP8.5 (2071–2100 minus 1971–2000) binned according to corresponding changes in *P* and PET. **b**, Same as **a**, for the EI. The associated density plot is shown in Supplementary Fig. 3.

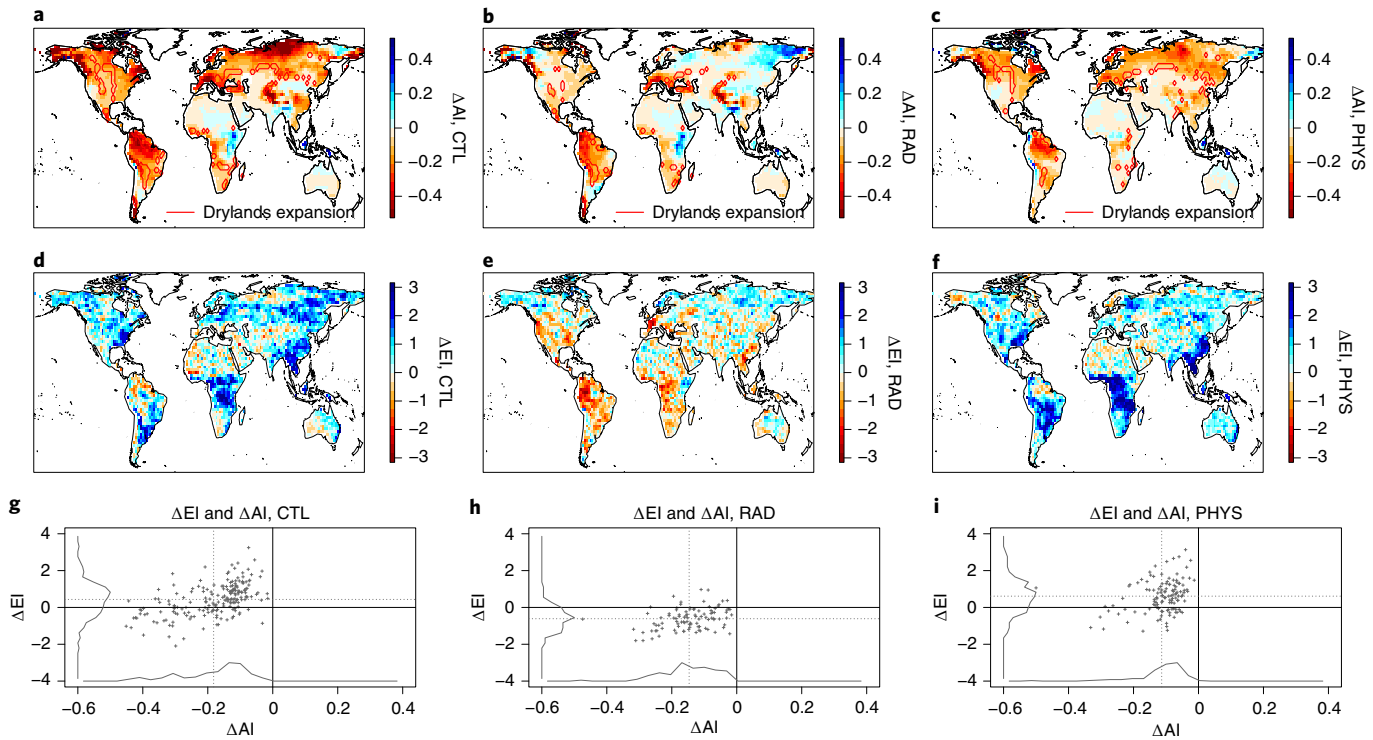

Fig. 4 | Plant physiology decouples AI and EI projections. a–**c**, Changes in AI in CTL (**a**), RAD (**b**) and PHYS (**c**) simulations; the red contour lines indicate drylands expansion under the AI definition. **d**–**f**, Changes in EI in CTL (**d**), RAD (**e**) and PHYS (**f**) simulations. **g**–**i**, Changes in EI versus AI in regions where AI-defined drylands expand (shown in **a**–**c**) in CTL (**g**), RAD (**h**) and PHYS (**i**) simulations. The dotted lines indicate the mean AI and EI values over these regions. The solid lines on the *x* axis and *y* axis show the distributions of EI and AI values (the values are normalized so that the maximum of the distribution has a value of 1 on the *y* axis for the AI and 0.1 on the *x* axis for the EI).

negative Δ*P*, the greater average ΔPET. This suggests that part of the increase in PET must actually be interpreted as a response to Δ*P*, mediated in part by land–atmosphere feedbacks[27,28].

The slight overall increase in the EI globally in Fig. 2b (+0.29) is thus consistent with the slight projected increase in land *P* (+0.15 mm d^{-1}, or +6.3%). The AI response (−0.13 globally in Fig. 2a) is dominated by the larger global PET increase (+0.66 mm d^{-1}, or +19%). The different sensitivities of the EI and the AI to contrasted *P* and PET changes thus explain some of the divergence in the AI and EI responses to climate change.

Physiological drivers of the AI–EI divergence

Differences in climatic sensitivity do not fully explain the discrepancy between AI and EI projections over drylands. A major forcing of the simulated ecohydrological response to greenhouse warming is the increase in plant water-use efficiency with increased atmospheric CO_2, which increases net primary productivity while reducing stomatal conductance[23,29,30], thus potentially modulating plant water constraints[31]. To better understand the role of vegetation physiology in the response of drylands, we analyse CMIP5 Earth System Model simulations that separate the

radiative effect of CO_2 on climate from its physiological effect on vegetation (Methods).

Projections for the control (CTL) simulations, which include both the radiative and physiological effects of four-time-increased CO_2, show a similar behaviour as the broader CMIP5 ensemble (Fig. 4a,d,g): widespread decrease in the AI and associated drylands expansion, even as the EI shows widespread increases, indicating denser and/or less water-limited vegetation. When only the radiative effect of CO_2 on climate is considered (RAD), however, the AI and EI projections are in better qualitative agreement, with mean changes of the same sign both globally (Fig. 4b,e) and over AI-defined expanded drylands specifically (Fig. 4h). In other words, suppressing the physiological effect of CO_2 substantially reduces the discrepancy between AI and EI changes. Consistently, the physiological effect of increased CO_2 (isolated in PHYS) induces a large EI increase (Fig. 4f), suggesting that EI changes in CTL (Fig. 4d) are dominated by plant physiology. The contrasted EI responses in PHYS and RAD predominantly reflect changes in LAI: as shown in previous studies[32,33], LAI increases in CMIP5 models are largely driven by CO_2 fertilization, especially in the tropics and subtropics, where climate change alone otherwise induces vegetation decrease (Supplementary Fig. 4a–c). While more muted, changes in water limitation show qualitatively consistent changes, with water limitation tending to increase in RAD and decrease in PHYS (Supplementary Fig. 4d–f). Increased atmospheric CO_2 thus reduces ecohydrological aridity both by increasing biomass and by reducing water limitation.

In addition to the EI increase, the response of vegetation to CO_2 in PHYS also leads to widespread AI decreases (Fig. 4c). These are driven both by decreases in P and by increases in PET, contributing, respectively, 25% and 75% of the total AI change (Supplementary Fig. 5 and Methods). Both are induced by land–atmosphere feedbacks caused by the decreases in plant transpiration occurring in models under higher atmospheric CO_2, as bulk stomatal conductance decreases (even as total LAI increases; Supplementary Fig. 4). While physiological feedbacks on surface climate have been analysed before[32,34–36], here we show that the combined effect on the AI is very large: the globally averaged AI decrease in PHYS represents 52% of that in CTL, leading to an apparent expansion in AI-defined drylands equivalent to 60% of that in CTL. As the EI otherwise increases (Fig. 4f), changes in the AI and EI in PHYS over new AI-defined drylands are of opposite signs (Fig. 4i). The physiological response of vegetation to CO_2 thus partially decouples atmospheric and ecohydrological aridity trends under climate change, as it simultaneously reduces ecohydrological aridity and enhances atmospheric aridity through associated land–atmosphere feedbacks. This divergence fundamentally undermines the justification for using the AI as a proxy for drylands expansion.

Projections of future drylands extent

Under the AI definition, the average global drylands area across our CMIP5 ensemble increases by 6% in the multimodel mean (from 40% to 46%; Fig. 5) and by 5.5% (from 42.9% to 48.4%) in the mean of individual model changes (+4.8% in the median). These results are qualitatively consistent with previous publications[7,10,13] (Methods). In contrast, under the EI-based definition of drylands, the global drylands extent remains essentially unchanged: −0.7% (from 35.8% to 35.1%) in the multimodel mean (−1.7% in the mean of model changes and −2.4% in the median), with regional contraction offsetting expansion (Fig. 2b). Despite larger model spread (Fig. 5), future changes in the EI remain smaller (−2.9% to +2.6%) than those in the AI (+3.7% to +7.2%) across all models. AI-based assessments thus lead to an overestimation of future global drylands expansion when compared with ecohydrological projections.

Climate models may underestimate present-day climate aridity in current drylands[10]; furthermore, vegetation projections from climate models often remain constrained by model configuration, allowing, for instance, interactive phenology locally but not changes in vegetation spatial distribution. We therefore also evaluate EI-based drylands changes in projections from three state-of-the-art Dynamic Global Vegetation Models (DGVMs), forced by multimodel climate projections under scenario RCP6.0 in phase 2b of the Inter-sectoral Impact Model Intercomparison Project (ISIMIP[37]; Methods).

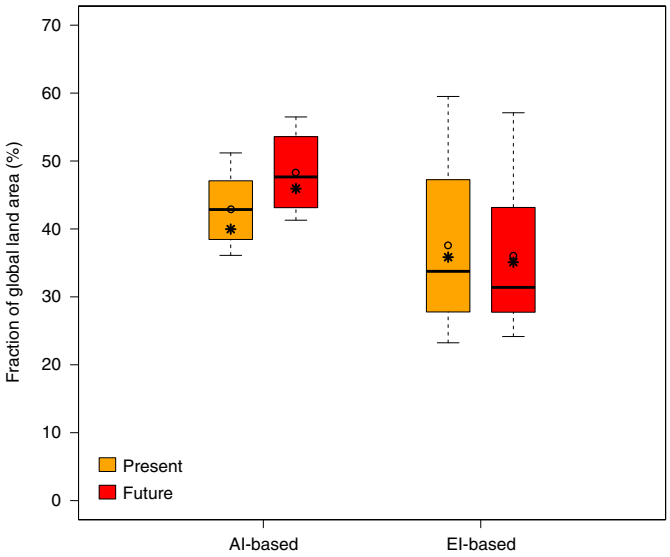

Fig. 5 | Changes in drylands area in CMIP5 models under the AI and EI definitions. Distribution of the global fraction of drylands in CMIP5 models in the present (1971–2000) and future (2071–2100, RCP8.5), based on either the AI definition (left) or the EI definition (right). The box edges represent the first and third quartiles of the CMIP5 distribution, the centre line represents the median, the dot represents the mean and the whiskers represent the entire range. The star indicates the drylands fraction estimated using the multimodel mean (shown in Fig. 2).

Across the climate model/DGVM ensemble, the EI-based global drylands area remains unchanged (−0.1% of global land from the multimodel/DGVM mean; +0.7% (−0.9%) from the mean (median) of individual model/DGVM changes; Fig. 6c). The spatial patterns are broadly similar to the CMIP5 results (Fig. 6a). Removing the CO_2 effect on vegetation leads to much more negative EI changes (Fig. 6b). Regions of drylands increase thus tend to show greater expansion (for example, central United States), and the associated increase in global drylands is larger (+3.2% of global land from the multimodel/DGVM mean; +3.1% (+2.7%) from the mean (median) of individual changes; Fig. 6c). The ISIMIP results thus confirm the CMIP5 results regarding the quasi-invariance of the global drylands extent to global warming and the key role of CO_2 fertilization in this response.

Discussion and conclusions

Even though the usual definition of drylands relies on the AI, here we showed that the modelled AI is actually a poor predictor of projected changes in drylands from climate model land surface outputs. Whereas AI projections indicate large future drylands expansion, EI projections suggest very limited areal changes in the global mean. This is consistent with previous studies showing the AI to be a negatively biased metric of modelled global land surface changes under greenhouse warming[19,20], despite its popularity as a climate impact metric[7–17]. Our study further highlights relevant mechanisms: AI-based assessments overemphasize the role of PET compared with P as a driver of ecohydrological impacts over land, do not account

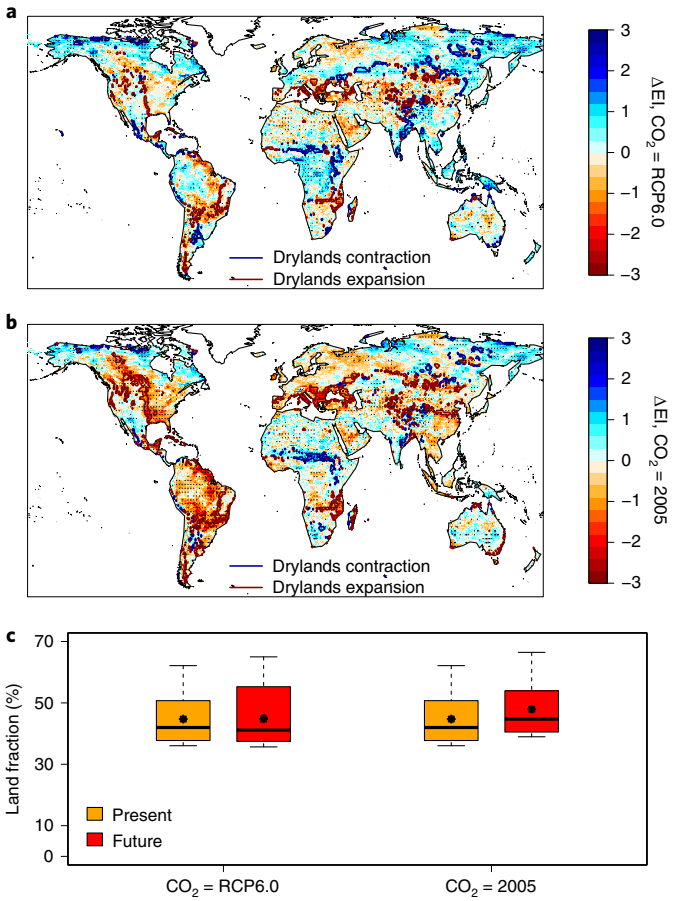

Fig. 6 | Changes in drylands in ISIMIP. a, Model mean change (across all combinations of DGVMs and climate models) in EI under the RCP6.0 scenario between the present (1971–2000) and future (2070–2099), with atmospheric CO_2 seen by vegetation following RCP6.0 values. The contour lines represent changes in drylands under the EI definition. **b**, Same as **a**, but with CO_2 concentrations seen by vegetation held constant after 2005. The stippling indicates where more than three-quarters of combinations of DGVMs and climate models agree on the sign of the change (for visibility, while the ISIMIP outputs are at a 0.5° × 0.5° resolution, the stippling is plotted at a 2° × 2° resolution). **c**, Distribution of drylands area (as a percentage of global land) in different DGVM/climate model combinations, in the present and future, with (left) and without (right) vegetation experiencing atmospheric CO_2 increase after 2005. The box plots have the same structure as in Fig. 5.

for the effect of CO_2 fertilization and neglect the role of land–atmosphere feedbacks associated with vegetation physiology in AI trends themselves. The latter result is consistent with similar issues identified in projections from other PET-based metrics[31]. Including a proposed correction[22] in PET calculations to account for plant stomatal responses to CO_2 does not resolve the discrepancy between the AI and EI drylands projections, highlighting fundamental issues with the AI beyond PET calculation (Supplementary Discussion 1 and Methods). We expect such issues to also apply in the latest modelling results of CMIP6.

While we did not seek here to explicitly evaluate AI and EI trends in observations, we note that the AI has predominantly decreased over land over the past 50 years[10], while vegetation has been increasing globally[38]. Over drylands specifically, little correlation is found between changes in the AI and vegetation density over recent decades[39]. A dominant role of land use or land management changes is found instead, consistent with a limited influence of ongoing climatic trends on drylands conditions[40,41]. Recent observations therefore do not seem to support the role of the AI as an indicator of drylands temporal dynamics either.

Climate models project widespread decreases in surface soil moisture[42], seemingly consistent with AI projections and thus drylands expansion[28] (Supplementary Fig. 8a). However, decreases in surface soil moisture are not consistently associated with increases in water limitation on transpiration in models: while changes in both quantities are spatially correlated ($r = -0.41$), 35% of the land surface shows decreases in surface soil moisture without increases in cor(SM,Tran) (Supplementary Fig. 8b). Decreasing soil moisture in wet environments (such as the tropics and high latitudes) may not directly impact transpiration; additionally, because of increased plant water-use efficiency under higher atmospheric CO_2, decreases in absolute soil water content may not translate to greater constraints on transpiration. Projected decreases in soil moisture in many midlatitude regions are also directly caused by climate-driven and CO_2-driven vegetation growth[43] and are thus not necessarily indicative of increased water stress in the models. These differences justify a focus on soil water limitation rather than absolute water content. Nevertheless, even tentatively defining drylands solely as regions with low surface soil moisture yields more modest drylands expansion than with the AI (+3%, Supplementary Fig. 9); a similar analysis applied to total-column soil moisture, which shows less negative projected changes than surface soil moisture[42], leads to a more modest increase (+1.9%, Supplementary Fig. 10). Finally, replacing cor(SM,Tran) with surface soil moisture in combination with LAI in an alternative EI (EI*; Supplementary Discussion 2) leads to no substantial drylands expansion, consistent with our initial results (+0.6% in the multimodel mean; Supplementary Fig. 11).

The realism of projected vegetation increases in climate models, however, may be questioned. On the one hand, available CO_2-enrichment experiments do show enhanced vegetation growth under elevated CO_2 (ref. [23]), with no clear evidence that models systematically overestimate this effect[44]; and model-simulated historical LAI trends are broadly consistent with the global vegetation increase observed in recent decades[38,45]. On the other hand, key limiting processes in a changing climate, such as increased water stress, nutrient limitation or increased fire risks[46,47], are represented simplistically in models or are entirely omitted. Models may thus overestimate future vegetation growth. We therefore design another alternative index to the EI that does not include LAI changes but focuses on precipitation and soil moisture limitation instead (EI′). The results obtained using this alternative index are still inconsistent with strong global drylands expansion (Supplementary Discussion 3 and Supplementary Figs. 12–14). We emphasize that, while model projections of future vegetation may be overestimated, evaluating the realism of such projections is not a goal of our study; rather, our study aims to accurately analyse and interpret the information that existing model projections provide, regardless of possible biases.

Land aridity is a complex, multidimensional hydroclimatic concept, of which the AI is but one metric. Similarly, the concept of drylands encompasses multiple climatic, hydrological and ecological characteristics[1]. A consequence of the AI-based definition of drylands and associated studies[7–17] is that both concepts have become somewhat conflated—further confounding their definition. Our study clarifies that the AI is best understood as a measure of atmospheric aridity (which does increase with climate change), while the concept of drylands is primarily based on land ecohydrological conditions. We use the EI as a tool to demonstrate that drylands show more nuanced changes under greenhouse warming, which cannot be equated with atmospheric aridity trends. However, we stress that the EI necessarily remains a simple metric, which does not encompass all drylands aspects, such as soil biogeochemistry and ecological composition[1]. Further work is needed to fully characterize the responses of all different facets of drylands. By further highlighting

the complex trends in the land–atmosphere system under climate change[19,20,28], our study joins calls for caution in the use of imprecise concepts such as aridity and drylands in climate impact studies, and for careful definition of the concepts and variables analysed[48]. In particular, our study highlights the dangers of relying on simple atmosphere-based metrics, such as the AI, as proxies to assess climate impacts on land systems. This approach is sometimes justified by the large structural uncertainties otherwise plaguing land surface outputs from climate models, such as soil moisture, runoff and vegetation[49] (for example, Fig. 5). However, here differences go beyond model spread: the AI-based assessments of future changes in drylands are qualitatively different from the modelled ecohydrological trends. Uncertainties and limitations in land model simulations undoubtedly complicate our assessment and interpretation of projected ecohydrological trends, and preclude high confidence in model EI projections. However, we argue that enough is known about ecohydrological processes that these uncertainties do not justify relying on a demonstrably flawed atmospheric proxy that is qualitatively at odds with these projections. Finally, we stress that our study does not question the many documented adverse impacts of climate change on different hydrological and biological land systems; however, we argue that an objective assessment of climate model projections indicates little evidence for global drylands expansion under anthropogenic climate change.

Online content

Any methods, additional references, Nature Research reporting summaries, source data, extended data, supplementary information, acknowledgements, peer review information; details of author contributions and competing interests; and statements of data and code availability are available at https://doi.org/10.1038/s41558-021-01007-8.

Received: 14 August 2020; Accepted: 12 February 2021;
Published online: 11 March 2021

References

1. D'Odorico, P. & Porporato, A. *Dryland Ecohydrology* (Springer, 2019).
2. Smith, W. K. et al. Remote sensing of dryland ecosystem structure and function: progress, challenges, and opportunities. *Remote Sens. Environ.* **233**, 111401 (2019).
3. Reynolds, J. F. et al. Global desertification: building a science for dryland development. *Science* **316**, 847–851 (2007).
4. Ahlström, A. et al. The dominant role of semi-arid ecosystems in the trend and variability of the land CO_2 sink. *Science* **348**, 895–899 (2015).
5. Middleton, N. & Thomas, D. S. G. *World Atlas of Desertification* 2nd edn (Wiley, 1997).
6. Budyko, M. I. & Miller, D. H. *International Geophysics Series: Climate and Life* Vol. 18 (Academic Press, 1974).
7. Feng, S. & Fu, Q. Expansion of global drylands under a warming climate. *Atmos. Chem. Phys.* **13**, 10081–10094 (2013).
8. Fu, Q. & Feng, S. Responses of terrestrial aridity to global warming. *J. Geophys. Res. Atmos.* **119**, 7863–7875 (2014).
9. Scheff, J. & Frierson, D. M. W. Terrestrial aridity and its response to greenhouse warming across CMIP5 climate models. *J. Clim.* **28**, 5583–5600 (2015).
10. Huang, J., Yu, H., Guan, X., Wang, G. & Guo, R. Accelerated dryland expansion under climate change. *Nat. Clim. Change* **6**, 166–171 (2016).
11. Huang, J., Yu, H., Dai, A., Wei, Y. & Kang, L. Drylands face potential threat under 2 °C global warming target. *Nat. Clim. Change* **7**, 417–422 (2017).
12. Park, C.-E. et al. Keeping global warming within 1.5 °C constrains emergence of aridification. *Nat. Clim. Change* **8**, 70–74 (2018).
13. Koutroulis, A. G. Dryland changes under different levels of global warming. *Sci. Total Environ.* **655**, 482–511 (2019).
14. Park, C. E. et al. Inequal responses of drylands to radiative forcing geoengineering methods. *Geophys. Res. Lett.* **46**, 14011–14020 (2019).
15. Wei, Y. et al. Drylands climate response to transient and stabilized 2 °C and 1.5 °C global warming targets. *Clim. Dyn.* **53**, 2375–2389 (2019).
16. Yao, J. et al. Accelerated dryland expansion regulates future variability in dryland gross primary production. *Nat. Commun.* **11**, 1665 (2020).
17. Berdugo, M. et al. Global ecosystem thresholds driven by aridity. *Science* **367**, 787–790 (2020).
18. Rajaud, A. & de Noblet-Ducoudré, N. Tropical semi-arid regions expanding over temperate latitudes under climate change. *Climatic Change* **144**, 703–719 (2017).
19. Yang, Y. et al. Disconnection between trends of atmospheric drying and continental runoff. *Water Resour. Res.* **54**, 4700–4713 (2018).
20. Greve, P., Roderick, M. L., Ukkola, A. M. & Wada, Y. The aridity index under global warming. *Environ. Res. Lett.* **14**, 124006 (2019).
21. Milly, P. C. D. & Dunne, K. A. Potential evapotranspiration and continental drying. *Nat. Clim. Change* **6**, 946–949 (2016).
22. Yang, Y., Roderick, M. L., Zhang, S., McVicar, T. R. & Donohue, R. J. Hydrologic implications of vegetation response to elevated CO_2 in climate projections. *Nat. Clim. Change* **9**, 44–48 (2019).
23. Norby, R. J. & Zak, D. R. Ecological lessons from free-air CO_2 enrichment (FACE) experiments. *Annu. Rev. Ecol. Evol. Syst.* **42**, 181–203 (2011).
24. Berg, A. & Sheffield, J. Soil moisture–evapotranspiration coupling in CMIP5 models: relationship with simulated climate and projections. *J. Clim.* **31**, 4865–4878 (2018).
25. Mahowald, N. et al. Projections of leaf area index in Earth system models. *Earth Syst. Dyn.* **7**, 211–229 (2016).
26. Sherwood, S. & Fu, Q. A drier future? *Science* **343**, 737–739 (2014).
27. Berg, A. et al. Land–atmosphere feedbacks amplify aridity increase over land under global warming. *Nat. Clim. Change* **6**, 869–874 (2016).
28. Berg, A. & Sheffield, J. Climate change and drought: the soil moisture perspective. *Curr. Clim. Change Rep.* **4**, 180–191 (2018).
29. Lavergne, A. et al. Observed and modelled historical trends in the water-use efficiency of plants and ecosystems. *Glob. Change Biol.* **25**, 2242–2257 (2019).
30. Friedlingstein, P. Carbon cycle feedbacks and future climate change. *Phil. Trans. R. Soc. A* **373**, 20140421 (2015).
31. Swann, A. L., Hoffman, F. M., Koven, C. D. & Randerson, J. T. Plant responses to increasing CO_2 reduce estimates of climate impacts on drought severity. *Proc. Natl Acad. Sci. USA* **113**, 10019–10024 (2016).
32. Lemordant, L., Gentine, P., Swann, A. S., Cook, B. I. & Scheff, J. Critical impact of vegetation physiology on the continental hydrologic cycle in response to increasing CO_2. *Proc. Natl Acad. Sci. USA* **115**, 4093–4098 (2018).
33. Berg, A. & Sheffield, J. Evapotranspiration partitioning in CMIP5 models: uncertainties and future projections. *J. Clim.* **32**, 2653–2671 (2019).
34. Cao, L., Bala, G., Caldeira, K., Nemani, R. & Ban-Weiss, G. Importance of carbon dioxide physiological forcing to future climate change. *Proc. Natl Acad. Sci. USA* **107**, 9513–9518 (2010).
35. Skinner, C. B., Poulsen, C. J. & Mankin, J. S. Amplification of heat extremes by plant CO_2 physiological forcing. *Nat. Commun.* **9**, 1094 (2018).
36. Kooperman, G. J. et al. Forest response to rising CO_2 drives zonally asymmetric rainfall change over tropical land. *Nat. Clim. Change* **8**, 434–440 (2018).
37. Frieler, K. et al. Assessing the impacts of 1.5 °C global warming—simulation protocol of the Inter-sectoral Impact Model Intercomparison Project (ISIMIP2b). *Geosci. Model Dev.* **10**, 4321–4345 (2017).
38. Zhu, Z. et al. Greening of the Earth and its drivers. *Nat. Clim. Change* **6**, 791–795 (2016).
39. He, B., Wang, S., Guo, L. & Wu, X. Aridity change and its correlation with greening over drylands. *Agric. For. Meteorol.* **278**, 107663 (2019).
40. Brandt, M. et al. Human population growth offsets climate-driven increase in woody vegetation in sub-Saharan Africa. *Nat. Ecol. Evol.* **1**, 0081 (2017).
41. Burrell, A. L., Evans, J. P. & De Kauwe, M. G. Anthropogenic climate change has driven over 5 million km^2 of drylands towards desertification. *Nat. Commun.* **11**, 3853 (2020).
42. Berg, A., Sheffield, J. & Milly, P. C. D. Divergent surface and total soil moisture projections under global warming. *Geophys. Res. Lett.* **44**, 236–244 (2017).
43. Mankin, J. S., Seager, R., Smerdon, J. E., Cook, B. I. & Williams, A. P. Mid-latitude freshwater availability reduced by projected vegetation responses to climate change. *Nat. Geosci.* **12**, 983–988 (2019).
44. Liu, Y. et al. Field-experiment constraints on the enhancement of the terrestrial carbon sink by CO_2 fertilization. *Nat. Geosci.* **12**, 809–814 (2019).
45. Zeng, Z. et al. Responses of land evapotranspiration to Earth's greening in CMIP5 Earth System Models. *Environ. Res. Lett.* **11**, 104006 (2016).
46. Peñuelas, J. et al. Shifting from a fertilization-dominated to a warming-dominated period. *Nat. Ecol. Evol.* **1**, 1438–1445 (2017).
47. Brodribb, T. J., Powers, J., Cochard, H. & Choat, B. Hanging by a thread? Forests and drought. *Science* **368**, 261–266 (2020).
48. Scheff, J., Seager, R., Liu, H. & Coats, S. Are glacials dry? Consequences for paleoclimatology and for greenhouse warming. *J. Clim.* **30**, 6593–6609 (2017).
49. Ault, T. R. On the essentials of drought in a changing climate. *Science* **368**, 256–260 (2020).

Methods

EI of drylands. Our criteria for defining the EI included simplicity (for example, the smallest number of variables possible), accessibility from usual climate model outputs and overlap with the AI-based definition under present-day climate. The EI of drylands is defined as

$$\mathrm{EI} = \mathrm{LAI} - (a \times \mathrm{cor}(\mathrm{SM}, \mathrm{Tran}) + b) \quad (1)$$

where LAI and cor(SM,Tran) are unitless, and a and b are parameters. The parameters are estimated by fitting the line $\mathrm{LAI} = a\mathrm{cor}(\mathrm{SM},\mathrm{Tran}) + b$ to the black contour line in Fig. 1e. The estimated values used in this study are $a = 4.72$ and $b = 0.15$. By design, drylands (regions in the present climate in which $\mathrm{AI} < 0.65$) then approximately correspond to regions where $\mathrm{EI} < 0$. As opposed to the AI, which is an index of atmospheric aridity, we consider the EI as an index of ecohydrological aridity: lower EI values correspond to more arid conditions from an ecohydrological standpoint (that is, to lower vegetation density and more water-limited vegetation). We used surface soil moisture here (variable mrsos from CMIP5) for simplicity, as it represents the same depth for all models (even if absolute moisture levels still vary between models). The spatial pattern and magnitude of cor(SM,Tran) are similar for surface and total soil moisture[50] (reflecting consistent interannual variability in both quantities).

CMIP5 simulations. We used publicly available simulations from CMIP5. Supplementary Table 1 lists the models analysed for the different experiments used in our study—using CMIP5 nomenclature: HIST, RCP8.5, 1pctCO_2 (renamed CTL in our study), esmFdbk1 (renamed RAD) and esmFixClim1 (renamed PHYS). To calculate multimodel means, the models were regridded to a common 2°×2° resolution.

Pre-industrial, historical and future climate simulations. HIST and RCP8.5 are simulations covering the historical period (1850–2005) and twenty-first century under a high-emissions scenario (2006–2100), respectively. We analyse 30-year periods in each, 1971–2000 and 2071–2100, respectively. CO_2 concentrations in the RCP8.5 scenario reach around 935 ppm by the year 2100. Only 12 models were available with the outputs necessary to calculate PET (see below), as well as surface soil moisture and transpiration, and for which LAI was computed interactively with climate (as opposed to being prescribed; Supplementary Table 1).

Experiments separating CO_2 physiological and radiative effects. CTL, PHYS and RAD are idealized single-forcing CMIP5 experiments for coupled carbon–climate Earth System models, meant to study carbon cycle feedbacks. More precisely, they are meant to separate the effect of atmospheric CO_2 increase on climate and the carbon cycle into the radiative effect of CO_2 on the atmosphere and the physiological effect of CO_2 on vegetation. In CTL, both the atmospheric model and the land surface scheme of a climate model are subjected to a 1% annual increase of atmospheric CO_2 starting from pre-industrial levels (284 ppm) and lasting 140 years (ending at 1,132 ppm). In PHYS, only the vegetation module experiences the increase in CO_2, while the atmosphere continuously experiences pre-industrial CO_2 levels. Conversely, in RAD, only the atmosphere experiences the increase in CO_2, while vegetation continuously experiences pre-industrial CO_2 levels. For our purposes, PHYS thus isolates the impact of CO_2 increase on climate and hydrology through the physiological effect of CO_2 on vegetation, while RAD isolates only the radiative effect of CO_2 increase. These simulations and the corresponding decomposition of CO_2 effects into physiological and radiative parts in CMIP5 models have been used in previous hydroclimate studies[31–33,35,36]. Eight models took part in these experiments; only four models provided both LAI and the necessary outputs to calculate PET (Supplementary Table 1). For each run, we analyse the first 20 years and the last 20 years of the simulations to obtain the corresponding changes.

ISIMIP simulations. Under phase 2b of ISIMIP[37], impact models from various sectors (for example, hydrology, vegetation, human health and biodiversity) were driven in a consistent modelling framework by climate projections from a set of climate models and climate scenarios from the CMIP5 experiment. The ISIMIP climate dataset covers the period from 1860 through to 2099 on a horizontal grid with 0.5°×0.5° resolution; where necessary, climate model output was spatially interpolated. The data were bias-corrected to ensure long-term statistical agreement with the observation-based dataset EWEMBI (E2OBS, WFDEI and ERAI data merged and bias-corrected for ISIMIP[37]) over the period 1960–1999, while also preserving projected absolute trends in temperature and relative trends in P and all other variables.

For our analysis, we use monthly LAI, soil moisture and transpiration outputs from three DGVMs forced by a set of four climate models (GFDL-ESM2M, HadGEM2-ES, IPSL-CM5A-LR and MIROC5). We computed annual means from monthly outputs. We focused on scenario RCP6.0 for future projections, as counterpart experiments without CO_2 change were available for that scenario (which was not the case for RCP8.5). Three DGVMs (ORCHIDEE, LPJ-GUESS and CARAIB) were available that included historical simulations and future projections with and without CO_2 change. In the historical simulations, CO_2 was prescribed according to historical values. For the historical period (1860–2005), historical land-use change was also prescribed. For RCP6.0 projections (both with and without CO_2 changes), land use was fixed at 2005 values; thus, the differences between present (1971–2000) and future (2071–2100) values focus on the impact of climate change (and CO_2 for simulations that include CO_2 change).

In the ISIMIP experiment, soil moisture outputs were not standardized to a common depth. The three DGVMs used here have different soil schemes and depths. We use the sum of the first nine layers in ORCHIDEE (equivalent to ~0.7 m deep) and the first layer in LPJ-GUESS (0.5 m); CARAIB had only one layer available, whose actual depth varies depending on rooting depth around the world, starting at 0.7 m.

Calculation of PET and AI. We use monthly outputs of P and of near-surface temperature, specific humidity, wind speed, surface pressure, and latent and sensible heat flux to calculate PET according to the Penman–Monteith equation (see below). The AI was then defined as the ratio of annual mean P to annual mean PET. Drylands expansion is then estimated as the increase in land fraction (not including Greenland and Antarctica) where $\mathrm{AI} < 0.65$ between 1971–2000 and 2071–2100; this yields an expansion of ~6% in the mean of the CMIP5 models we analysed, consistent with previous studies[7,10,13] (note that Huang et al.[10] apply a bias correction to AI calculations from CMIP5 model simulations, which results in larger drylands expansion in their analysis, up to +23%; however, their non-corrected values are also on the order of +6%).

PET represents the evaporative demand of the air near the surface. To calculate PET, we used the open-water formulation, as in Milly and Dunne[21]. This assumes that stomatal resistance is zero (and thus doesn't change over the course of the twenty-first century); it also assumes an aerodynamic roughness of the surface of 0.00137 m (consistent with open water). It computes PET (mm d^{-1}) as:

$$\lambda\mathrm{PET} = \frac{sR_\mathrm{n} + 6.43(1 + 0.53u)\gamma D}{s + \gamma},$$

where s is the gradient of the saturation vapour pressure with respect to temperature (Pa K^{-1}), R_n is net radiation minus the ground heat flux (which was calculated as the sum of latent and sensible heat flux), γ is the psychrometric constant (Pa K^{-1}), u is the wind speed at 2 m height (m s^{-1}), D is the vapour pressure deficit of the air at 2 m height (the difference between the saturated vapour pressure and the actual vapour pressure (Pa)) and λ is the latent heat of vaporization (J kg^{-1}), which is calculated as a function of air temperature[21].

We also calculate PET using the formulation proposed by Yang et al.[22] to account for changes in stomatal resistance. It is based on the 'FAO-56 reference crop' formulation, which was modified to include changes in stomatal conductance as a function of atmospheric CO_2 (estimated from CMIP5 climate projections)[22]:

$$\mathrm{PET} = \frac{0.408sR_\mathrm{n} + \gamma\frac{900}{T+273}uD}{s + \gamma\{1 + u[0.34 + 2.4\times10^{-4}([\mathrm{CO_2}] - 300)]\}},$$

where T is the 2 m temperature and $[CO_2]$ is the atmospheric CO_2 concentration (in ppmv).

Decomposition of P/PET changes in the PHYS experiment. According to error propagation rules, the fractional change in $\mathrm{AI} = P/\mathrm{PET}$ can be approximated by the fractional change in P and in PET as follows:

$$\frac{\Delta\left(\frac{P}{\mathrm{PET}}\right)}{\frac{P}{\mathrm{PET}}} \approx \frac{\Delta P}{P} - \frac{\Delta\mathrm{PET}}{\mathrm{PET}},$$

where Δ refers to the future-minus-present change and the values in the denominator are present-day means. Thus, we have:

$$\Delta\left(\frac{P}{\mathrm{PET}}\right) \approx \frac{\Delta P}{P}\frac{P}{\mathrm{PET}} - \frac{\Delta\mathrm{PET}}{\mathrm{PET}}\frac{P}{\mathrm{PET}};$$

that is, the change in P/PET, Δ(P/PET), can be approximated by the difference between a P-change-induced term:

$$\frac{\Delta P}{P}\frac{P}{\mathrm{PET}}$$

and a PET-change-induced term:

$$\frac{\Delta\mathrm{PET}}{\mathrm{PET}}\frac{P}{\mathrm{PET}}.$$

We compute area-weighted averages of each term in experiment PHYS. We calculate the global change in P/PET to be −0.071 (unitless); the P-change-induced term and PET-change-induced term are −0.019 and +0.059, respectively (thus, their difference is −0.078). We therefore assess the change in AI in PHYS attributable to changes in P to be $1.9/7.8 \approx 25\%$; and the change in AI attributable to changes in PET, $5.9/7.8 \approx 75\%$.

Data availability

All climate model simulations used in the Article are from CMIP5 and are publicly available—for instance, at https://esgf-node.llnl.gov/search/cmip5/. All ISIMIP simulations are freely available as well—for example, at https://esg.pik-potsdam.de/search/isimip/. All calculated data generated from these sources are available from the corresponding author upon request.

Code availability

The custom R code written to read and analyse the data and generate the figures is available on GitHub at https://doi.org/10.5281/zenodo.4490414 (ref. [51]).

References

50. Berg, A. & Sheffield, J. Historic and projected changes in coupling between soil moisture and evapotranspiration (ET) confounded by the role of different ET components. *J. Geophys. Res. Atmos.* **124**, 5791–5806 (2019).
51. Berg, A. & McColl, K. R code for 'No global drylands expansion under greenhouse warming'. *Zenodo* https://doi.org/10.5281/zenodo.4490414 (2021).

Acknowledgements

We thank the World Climate Research Programme's Working Group on Coupled Modelling, which is responsible for CMIP, and we thank the climate modelling groups (listed in Supplementary Table 1 of this paper) for producing and making available their model output. For CMIP, the US Department of Energy's Program for Climate Model Diagnosis and Intercomparison provides coordinating support and led the development of software infrastructure in partnership with the Global Organization for Earth System Science Portals. For their roles in producing, coordinating and making available the ISIMIP input data and impact model output, we thank the modelling groups, the ISIMIP sector coordinators and the ISIMIP cross-sectoral science team for the Biomes sectors. K.A.M. acknowledges funding from a Winokur Seed Grant in Environmental Sciences from the Harvard University Center for the Environment.

Author contributions

A.B. and K.A.M. designed the study. A.B. conducted the analysis and wrote the manuscript. K.A.M. advised on the interpretation of the results and contributed to the manuscript preparation.

Competing interests

The authors declare no competing interests.

Additional information

Supplementary information The online version contains supplementary material available at https://doi.org/10.1038/s41558-021-01007-8.

Correspondence and requests for materials should be addressed to A.B.

Peer review information *Nature Climate Change* thanks Peter Greve, Congbin Fu and the other, anonymous, reviewer(s) for their contribution to the peer review of this work.

Reprints and permissions information is available at www.nature.com/reprints.

nature portfolio

https://doi.org/10.1038/s41558-021-01007-8

Supplementary information

No projected global drylands expansion under greenhouse warming

In the format provided by the authors and unedited

Supporting Information for

No projected global drylands expansion under greenhouse warming

Alexis Berg[1], Kaighin A. McColl[1,2]

[1] Harvard University, Department of Earth and Planetary Sciences, MA, USA

[2] Harvard University, School of Engineering and Applied Sciences, MA, USA

Content:

Model	Institution	HIST and RCP8.5	CTL, RAD, and PHYS (i.e., 1pctCO2, esmFdbk1, esmFixclim1)
bcc-csm1-1	Beijing Climate Center, China Meteorological Administration	✓	
bcc-csm1-1-m	Beijing Climate Center, China Meteorological Administration	✓	
CESM1-BGC	National Science Foundation, Department of Energy, National Center for Atmospheric Research		✓
CESM1-CAM5	National Science Foundation, Department of Energy, National Center for Atmospheric Research	✓	
CanESM2	Canadian Centre for Climate Modelling and Analysis	✓	✓
GFDL-ESM2G	Geophysical Fluid Dynamics Laboratory	✓	
GFDL-ESM2M	Geophysical Fluid Dynamics Laboratory	✓	✓
INMCM4	Institute for Numerical Mathematics	✓	
IPSL-CM5A-LR	Institut Pierre-Simon Laplace	✓	✓
IPSL-CM5A-MR	Institut Pierre-Simon Laplace	✓	
IPSL-CM5B-LR	Institut Pierre-Simon Laplace	✓	
MIROC-ESM	Japan Agency for Marine-Earth Science and Technology, Atmosphere and Ocean Research Institute (The University of Tokyo), and National Institute for Environmental Studies	✓	
MIROC-ESM-CHEM	Japan Agency for Marine-Earth Science and Technology, Atmosphere and Ocean Research Institute (The University of Tokyo), and National Institute for Environmental Studies	✓	

Supplementary Table 1: List of CMIP5 models used in this study (see ref[1] in this document for more information on details and protocols of the different simulations). These models were selected on the basis of the availability of all the necessary monthly outputs used in our analysis (variables involved in the calculation of PET (Methods), surface soil moisture, transpiration, LAI).

Supplementary Discussion 1:

Impact of PET CO_2-correction on AI/EI discrepancy

One known issue in the calculation of the Aridity Index (and other PET-based metrics) lies in the computation of future PET: by neglecting future changes in plant stomatal resistance under higher atmospheric CO_2 (as those are typically not provided in climate model outputs), PET projections overestimate evaporative demand[2]. In our own initial AI calculations, we have also neglected changes in stomatal conductance, consistent with prior studies.

However, Yang et al.[3] recently provided a way to remedy this issue and include changes in stomatal resistance in calculations of future PET (Methods). They argue that this correction reduces the gap between PET-based metrics and hydrological projections within climate models: for instance, they are able to retrieve model-simulated trends in global runoff from calculations based on changes in P/PET. Following their approach in our analysis, however, does not resolve the discrepancy between AI- and EI-based projected changes in drylands: while the increase in AI-defined drylands area in the multi-model mean is reduced (+3.5%; Fig. S6), as projected PET increases are smaller, it is still inconsistent with changes in EI, both globally and in many regions (Fig. S7). Thus, the proposed PET correction does not fully remedy the fundamental issues described in our study regarding the use of AI as a drylands metric under a warming climate.

Supplementary Discussion 2:

An alternative Ecohydrological Index (EI*) based on absolute soil moisture instead of soil moisture limitation

We argue (see discussion section in main text) that soil moisture limitation is a more relevant metric for characterizing drylands in climate change projections than absolute soil moisture. Nevertheless, to test the sensitivity of our results to plausible different choices of variables, we design an alternative index to EI, called EI*, in which we replace soil moisture limitation (cor(SM,Tran)) by absolute surface soil moisture (mrsos; Fig. S11). EI* is thus based on LAI and mrsos. To design EI*, we proceed as for EI: we bin AI as a function of mrsos and LAI and seek a simple

relationship between mrsos and LAI that corresponds to AI<0.65. For EI, given the shape of the AI<0.65 domain in the LAI/cor(SM,Tran) space, a linear relationship between LAI and cor(SM,Tran) could be established to delineate the AI<0.65 domain and define EI. However, given the shape of the AI<0.65 domain in the mrsos/LAI space (black contour line on Fig.S11e), absolute thresholds on mrsos and LAI were used instead to approximate AI-defined drylands: LAI=2 and mrsos=16 $kg.m^{-2}$. The corresponding index EI* is calculated as follows:

- for a pixel i,j (i and j representing longitude and latitude, respectively) with values $LAI_{i,j}$ and $mrsos_{i,j}$, if $LAI_{i,j}$ and $mrsos_i$ both fall below their respective thresholds, $EI^*_{i,j}$ is defined as $(LAI_{i,j}-2)+ (mrsos_{i,j}-16)/10$, so that its value is negative;
- if $LAI_{i,j}$ and $mrsos_{i,j}$ both fall above the thresholds, $EI^*_{i,j}$ is also defined as the sum of $(LAI_{i,j}-2)+ (mrsos_{i,j}-16)/10$; thus its value is positive.
- in other cases (when one value falls above its threshold but not the other), $EI^*_{i,j}$ is defined as max(1e-3, $(LAI_{i,j}-2)+ (mrsos_{i,j}-16)/10$); its value is thus also positive.

Thus $EI^*_{i,j}$ is only negative if both $LAI_{i,j}$ and $mrsos_{i,j}$, are below their respective thresholds; that is, as for EI, EI*-based drylands are defined as EI*<0. Note that mrsos is divided by 10 so that LAI and mrsos contribute broadly comparable values. As discussed in the main text and shown on Fig. S11h, across models EI*-defined drylands show no substantial increase in climate change projections.

Supplementary Discussion 3:

An alternative Ecohydrological Index (EI') based on precipitation instead of Leaf Area Index

To account for uncertainties in climate model vegetation projections (which are potentially overestimated), we design another alternative Ecohydrological Index (EI'), in which LAI is replaced by mean annual precipitation P (Fig. S12). EI' thus only relies on precipitation and soil moisture limitation. EI' is established similarly to EI, by establishing a linear relationship between P and cor(SM,Tran) delineating the AI<0.65 domain on the binned plot of AI as a function of P and cor(SM,Tran) (Fig. 12e). The combination of these two variables allows accurately capturing AI-defined

drylands, similar to the initial EI metric. Even without considering projected vegetation increases, changes in EI' in RCP8.5 climate change projections are still inconsistent with strong global drylands expansion (+2.1% in the change of multimodel mean; -0.2% in the mean of model changes; -2.1% in the median of model changes; Fig. S13). Further, this index counts as expanding drylands some Northern Hemisphere regions (e.g., North America) without any precipitation decrease, but with both LAI increases (Fig. 2) and increased soil moisture limitation (Fig. S14). Such changes can be interpreted as enhanced vegetation growth depleting soil moisture to the point of increased water limitation, even as precipitation remains constant[4]. We contend that such a situation does not correspond to the conventional understanding of "drylands expansion" driven by climatic changes, and should thus not be counted as such. This further demonstrates the importance of accounting for LAI changes when assessing drylands dynamics, as we do with the EI, lest some regions be misclassified as future drylands.

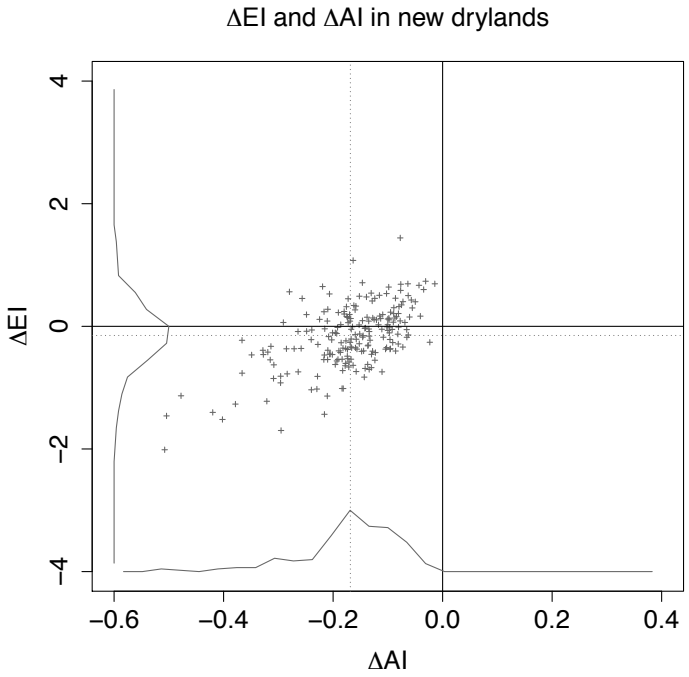

Figure S1: changes in Ecohydrological Index versus Aridity Index between 1971-2000 and 2071-2000 (in RCP8.5 scenario) in regions where AI-defined drylands expand (see contour lines on Fig.2a). Gray dotted lines indicate the mean of AI and EI values. Gray lines on the x-axis and y-axis give an indication of the distribution of EI and AI values (values are normalized so that the maximum of the distribution has a value of 1 on the y-axis for AI, and 0.1 on the x-axis for EI).

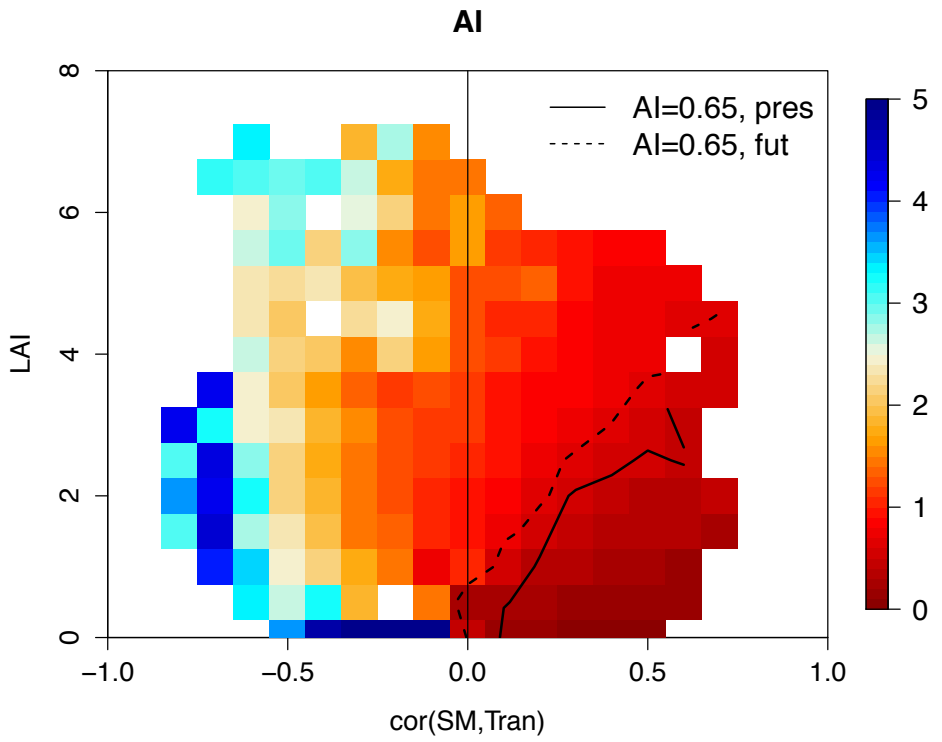

Figure S2: Model mean AI binned as a function of mean cor(SM,Tran) and mean LAI, in the future (2071-2100, RCP8.5 scenario). The dotted contour line delineates values lower than 0.65, i.e., AI-defined drylands. The full line show the same contour line, but for present-day climate (i.e., from Fig.1e).

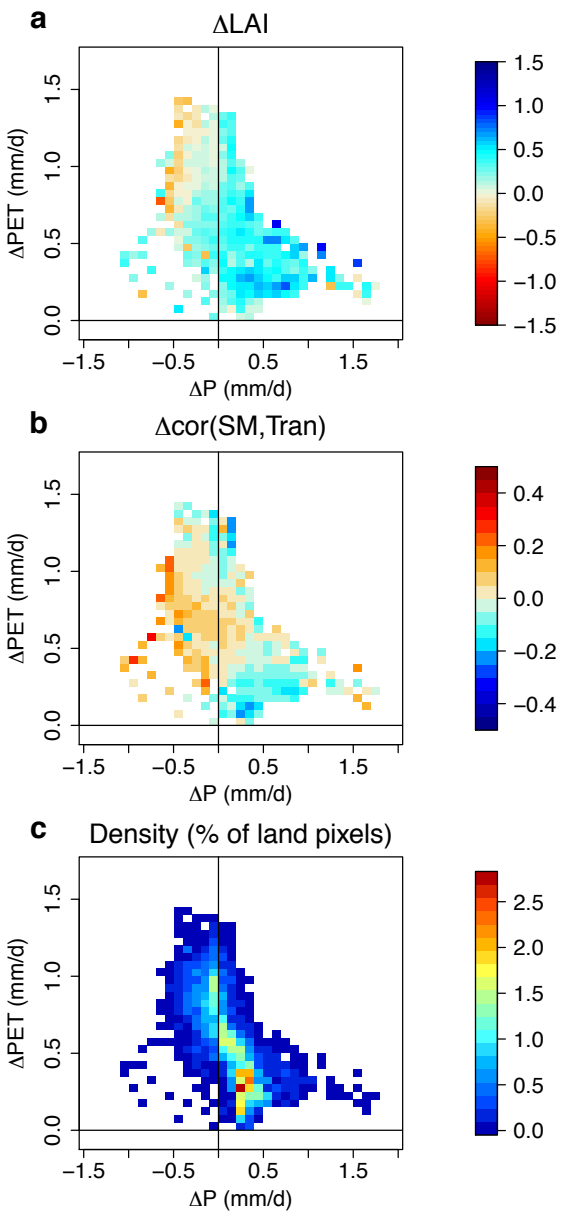

Figure S3: Changes in (a) Leaf Area index and (b) soil moisture-transpiration correlations in CMIP5 models in RCP8.5 (2071-2100 minus 1971-2000) binned according to corresponding changes in annual P and PET; (c) Density plot associated with Fig. 3 and panels (a) and (b).

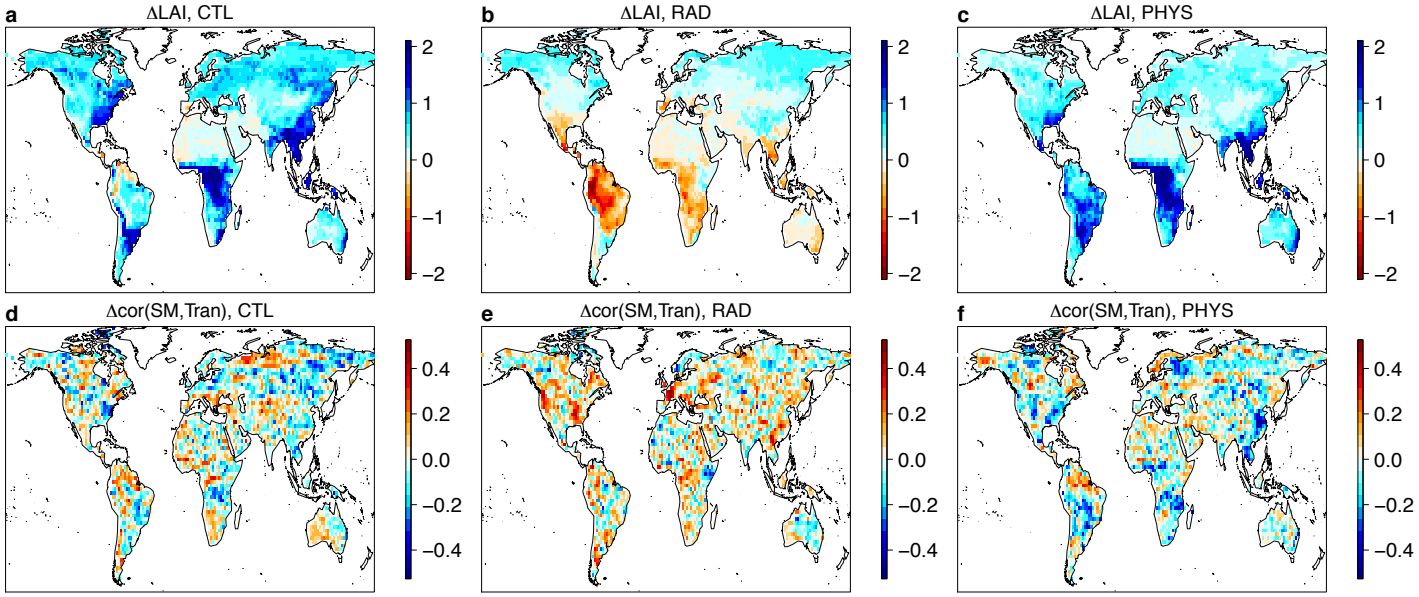

Figure S4: (a-c) changes in mean annual Leaf Area Index in CTL, RAD and PHYS simulations under a four-time increase in atmospheric CO_2; (c-e): Changes in correlation between mean annual surface soil moisture and transpiration in CTL, RAD PHYS simulations.

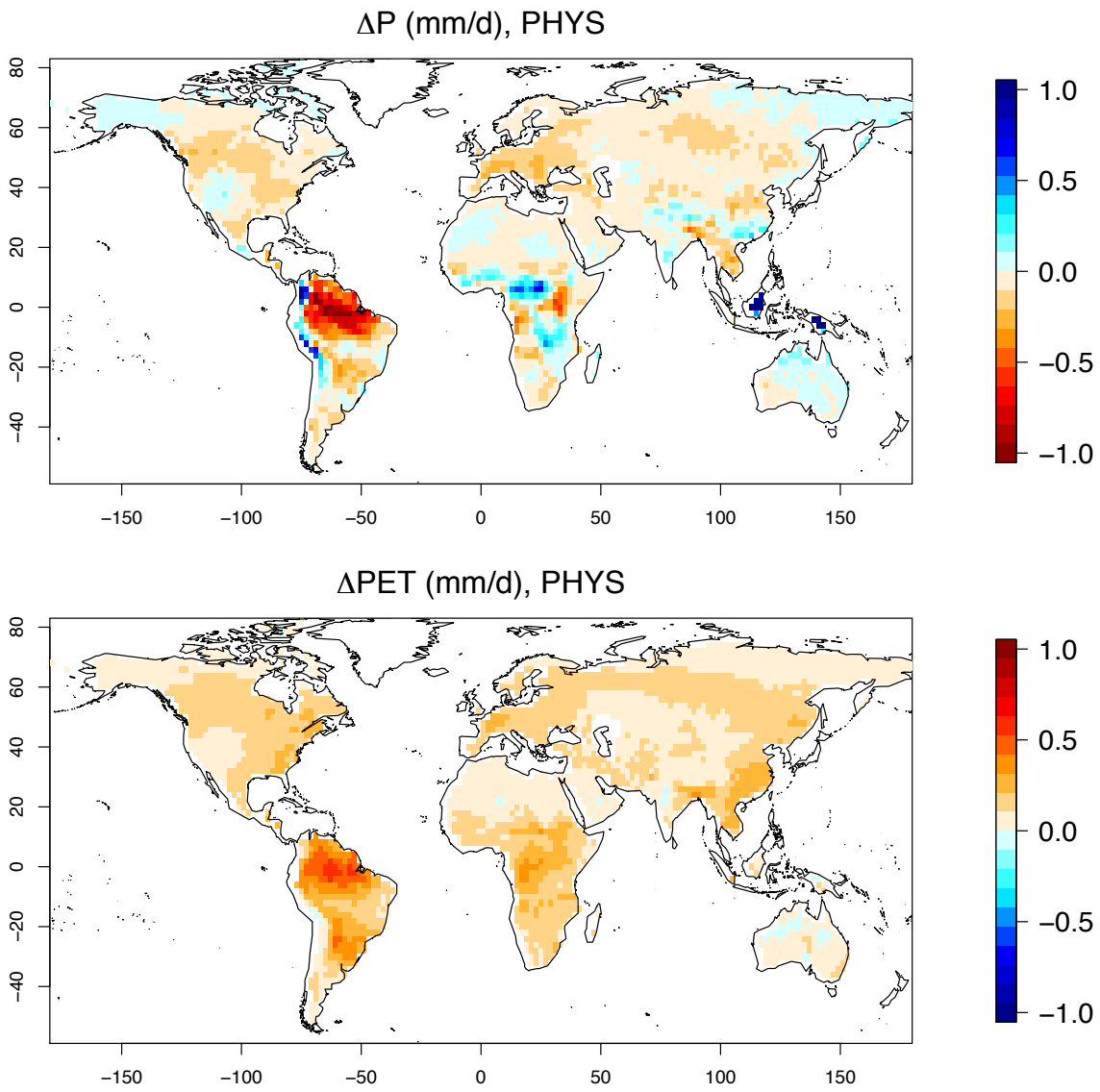

Figure S5: Model mean change in mean annual precipitation (top) and potential evapotranspiration (bottom) in the PHYS simulation (note the different color scales).

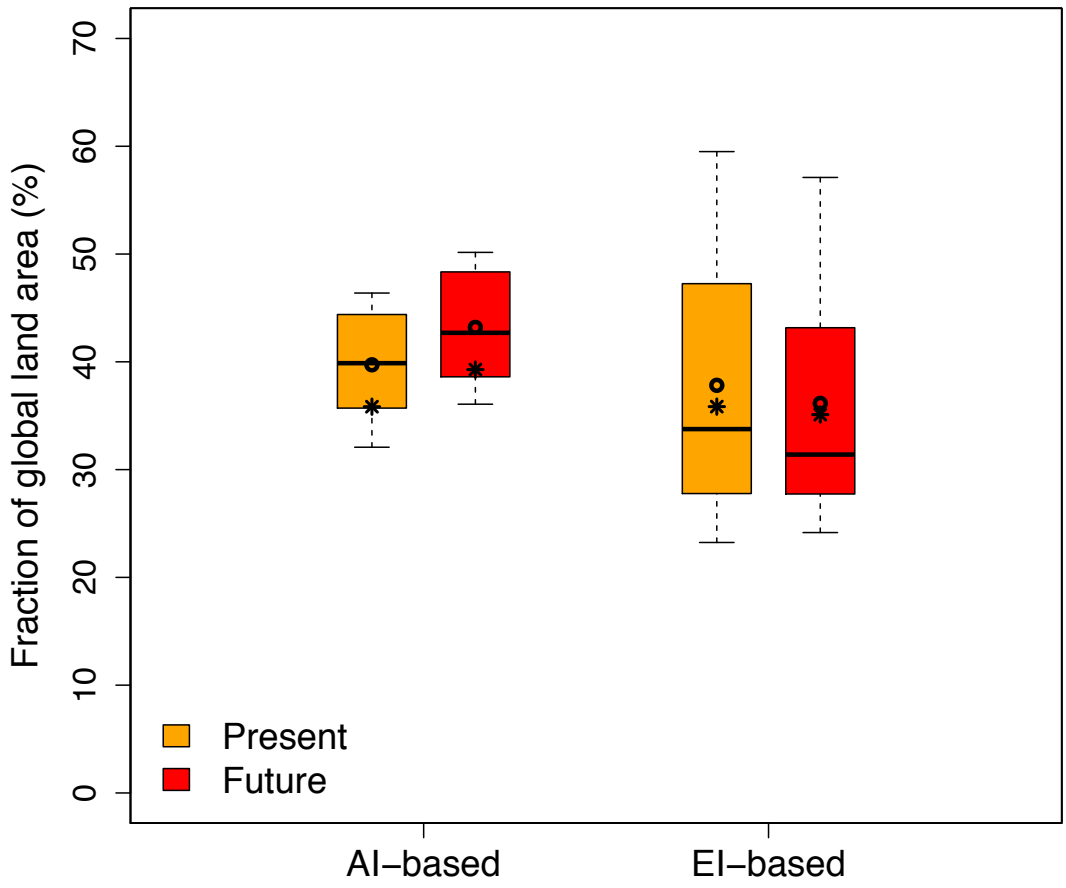

Figure S6: Same as Figure 5, but with AI calculations including a corrected version of PET calculation that accounts for changes in stomatal conductance induced by increased atmospheric CO_2 (Methods).

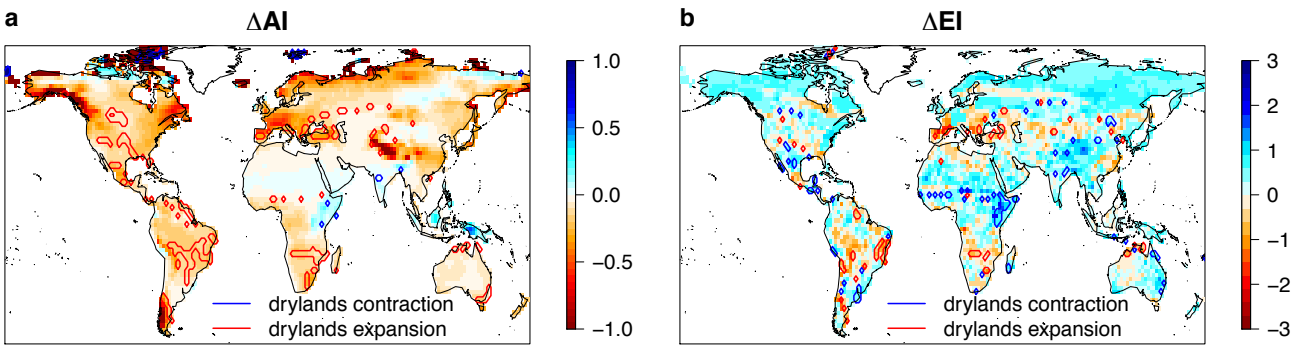

Figure S7: Same as panels (a) and (b) from Fig.2, but with AI calculations in (a) including a corrected version of PET calculation that accounts for changes in stomatal conductance induced by increased atmospheric CO_2 (Methods).

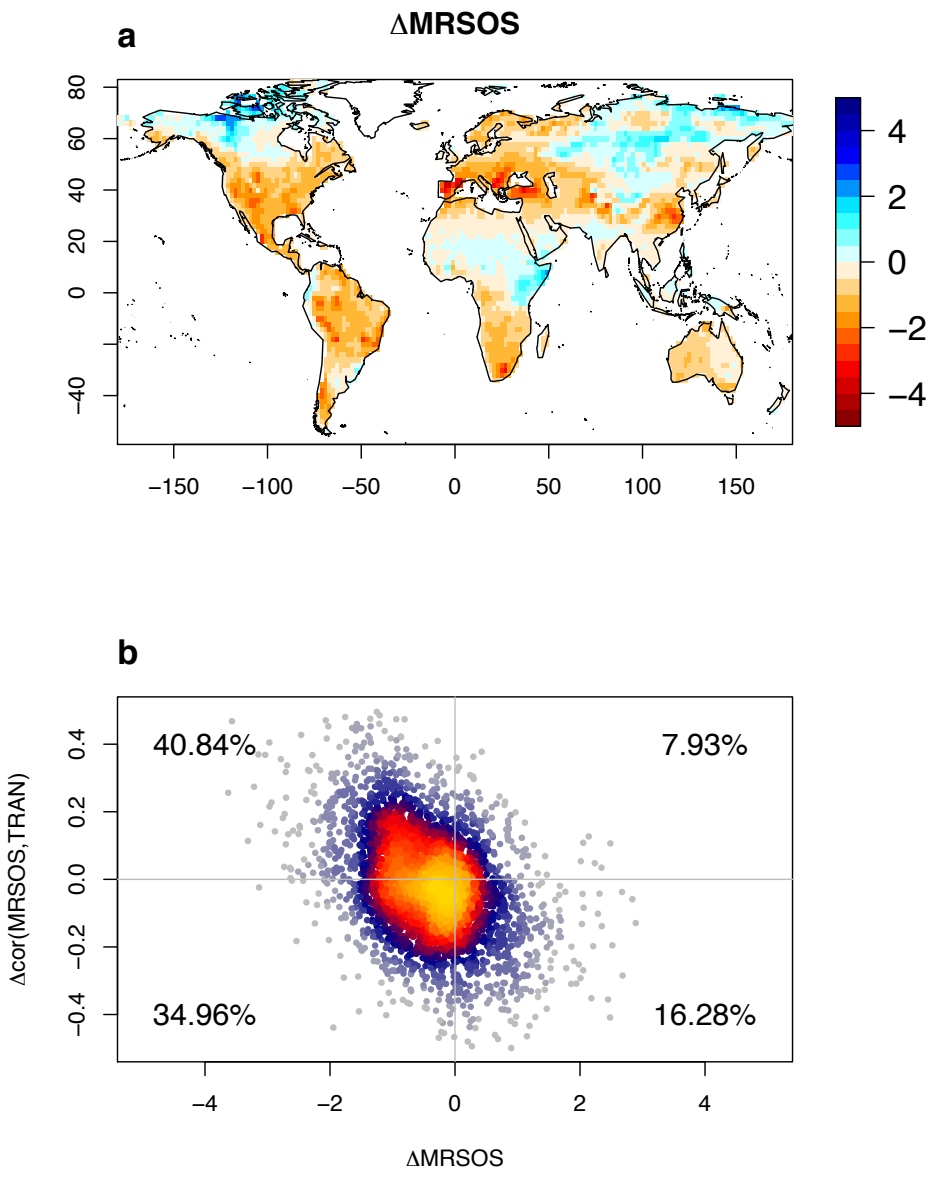

Figure S8: (a) Change in mean annual surface soil moisture (mrsos; kg/m²) between 1971-2000 and 2071-2100 in RCP8.5 scenario in the models analyzed in this study; (b) Scatterplot of the change in mean annual surface soil moisture (x-axis) and the change in the correlation between annual transpiration and annual surface soil moisture (y-axis); colors give an indication of the density of points. Numbers indicate the percentage of the land surface that falls in each quadrant (defined by the axis lines).

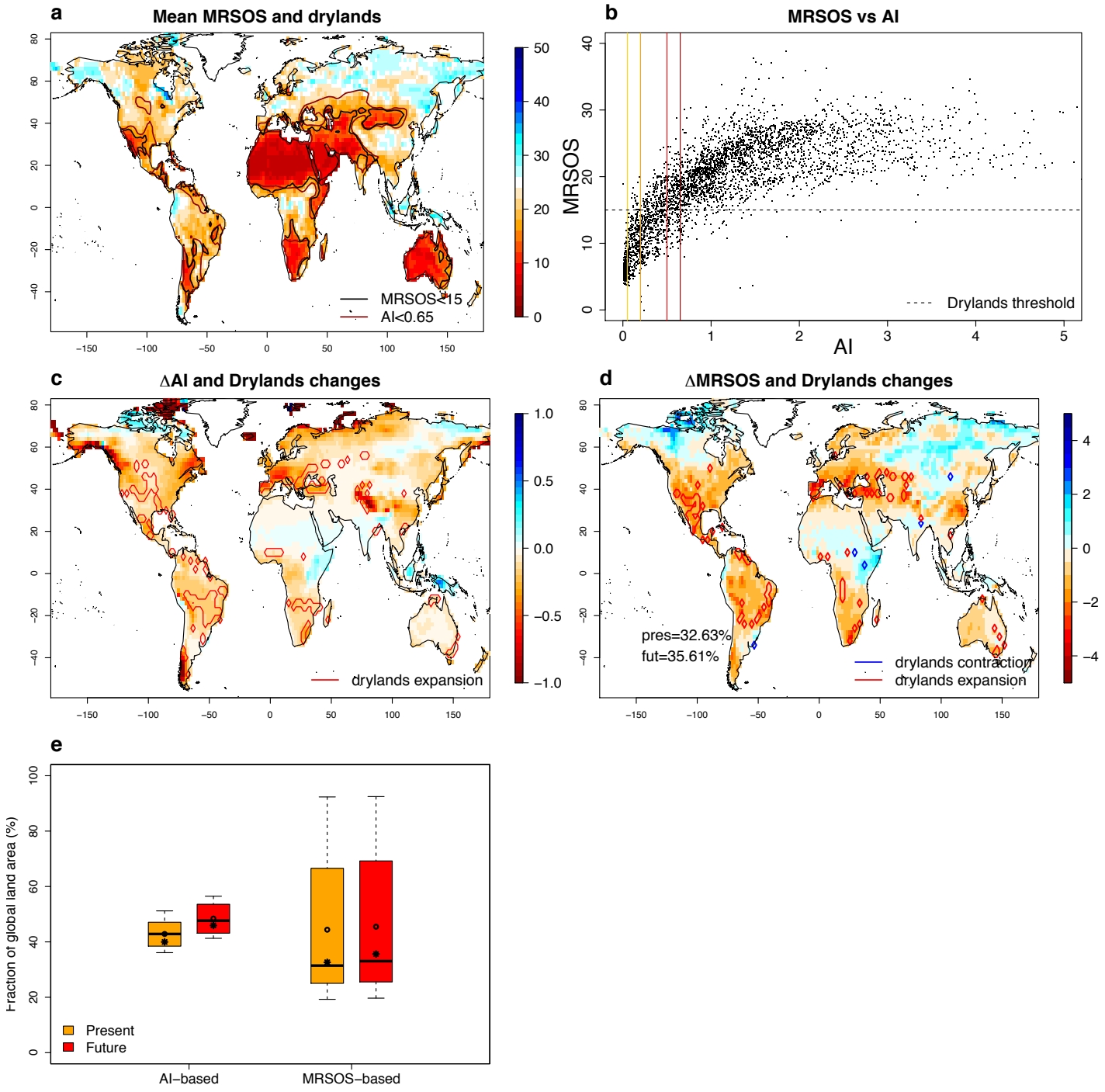

Figure S9: (a) Mean annual surface soil moisture (mrsos; kg/m²) over 1971-2000; contour lines indicate AI-defined drylands (in dark red) and drylands defined based on threshold of mrsos (black), chosen as mrsos=15 kg.m⁻² based on (b); note the spatial discrepancy between both definitions, as mrsos values do not strictly overlap with AI values; (b) Mean annual surface soil moisture (mrsos; kg/m²) over 1971-2000 against mean AI; vertical color lines correspond to different levels of drylands aridity (see

caption of Fig. 1); horizontal dotted line is a threshold of surface soil moisture value to approximate AI-based drylands, based on the intersect of the vertical AI=0.65 line with the data points ; (c) Mean change in Aridity Index between 1971-2000 and 2071-2100 in RCP8.5 scenario; contour lines indicate changes in drylands defined based on AI; (d) Change in surface soil moisture between 1971-2000 and 2071-2100 in RCP8.5 (same as panel (a) from Fig. S8); contour lines indicate changes in drylands based on changes in mrsos and the threshold from panel (b); percentages indicate the fraction of land area then considered as drylands in the present (pres) and the future (fut); (e) As on Figure 5, distribution of global fraction of drylands across CMIP5 models in the present (1971-2000) and future (2071-2100, RCP8.5), based either on the AI definition (left) or the mrsos-based definition (right); note the wide distribution for the latter, reflecting the large spread in soil moisture values across CMIP5 models.

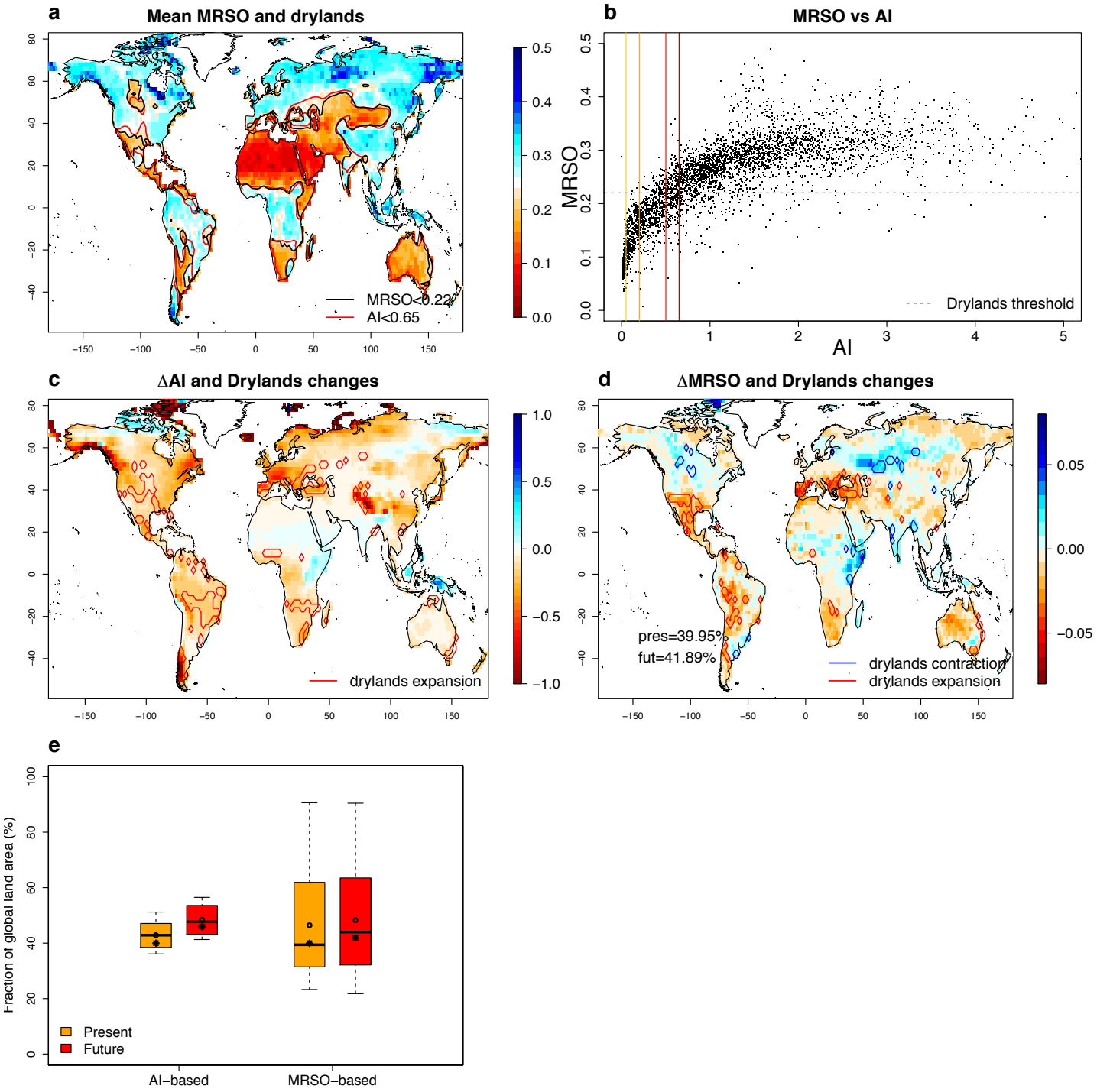

Figure S10: (a) Mean annual total-column soil moisture (mrso), normalized by soil depth in each model (i.e., volumetric soil moisture, expressed in m^3/m^3) over 1971-2000; contour lines indicate AI-defined drylands (in red) and drylands defined based on a threshold of mrso, chosen as mrso=0.22 $m^3.m^{-3}$, based on (b); note the spatial discrepancy between both definitions, as mrso values do not strictly overlap with AI values; (b) Mean volumetric total-column annual soil moisture over 1971-2000 against

mean AI; vertical color lines correspond to different levels of drylands aridity (see caption of Fig. 1); horizontal dotted line is a threshold of total-column volumetric soil moisture value to approximate AI-based drylands; (c) Mean change in Aridity Index between 1971-2000 and 2071-2100 in RCP8.5 scenario; contour lines indicate changes in drylands defined based on AI. (d) Change in volumetric total-column soil moisture between 1971-2000 and 2071-2100 in RCP8.5; contour lines indicate changes in drylands based on changes in mrso and the threshold from panel (b); percentages indicate the fraction of land area then considered as drylands in the present (pres) and the future (fut); (e) As on Figure 5, distribution of global fraction of drylands across CMIP5 models in the present (1971-2000) and future (2071-2100, RCP8.5), based either on the AI definition (left) or the mrso-based definition (right); note the wide distribution for the latter, reflecting the large spread in soil moisture values across CMIP5 models.

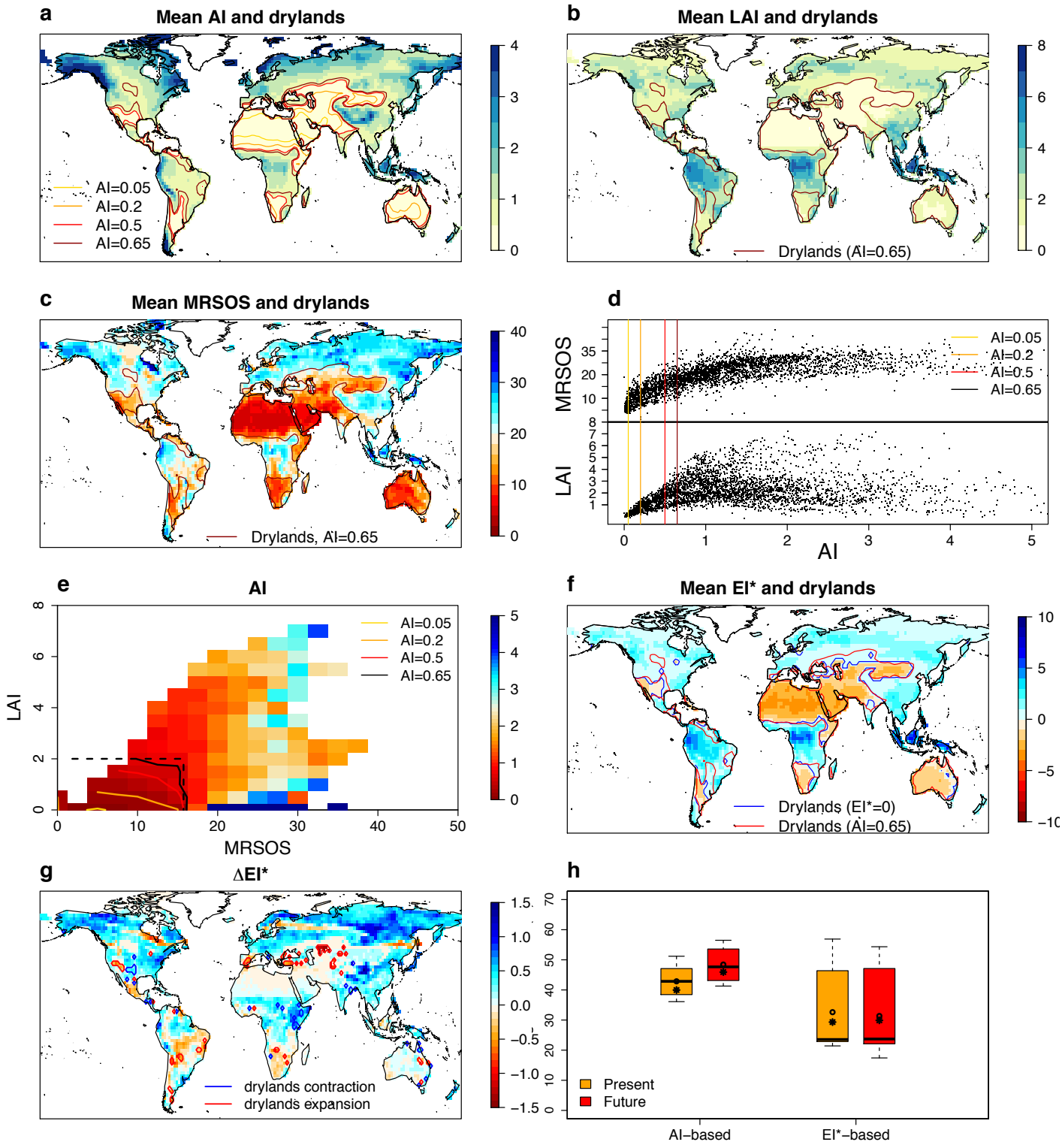

Figure S11: (a) Multi-model mean Aridity Index (AI) and corresponding drylands classification over 1971-2000 (see caption of Fig. 1); (b) Multi-model mean annual Leaf Area Index (LAI); contour line represent drylands according to the AI-based definition (AI<0.65); (c) Multi-model mean surface soil moisture (mrsos, kg.m^{-2}); contour line as in (b); (d) Relationship over global land between AI and LAI or mrsos, from (a), (b) and

(c), with vertical lines corresponding to AI thresholds denoted in (a); (e) Multi-model mean AI binned as a function of mean mrsos and mean LAI; (f) Corresponding multi-model mean Ecohydrological Index EI; contour lines indicate drylands based on the AI and EI* definition; (g) Change in the Ecohydrological Index EI*, with corresponding changes in drylands; (h) As on Figure 5, distribution of global fraction of drylands across CMIP5 models in the present (1971-2000) and future (2071-2100, RCP8.5), based either on the AI definition (left) or the alternative EI* definition (right).*

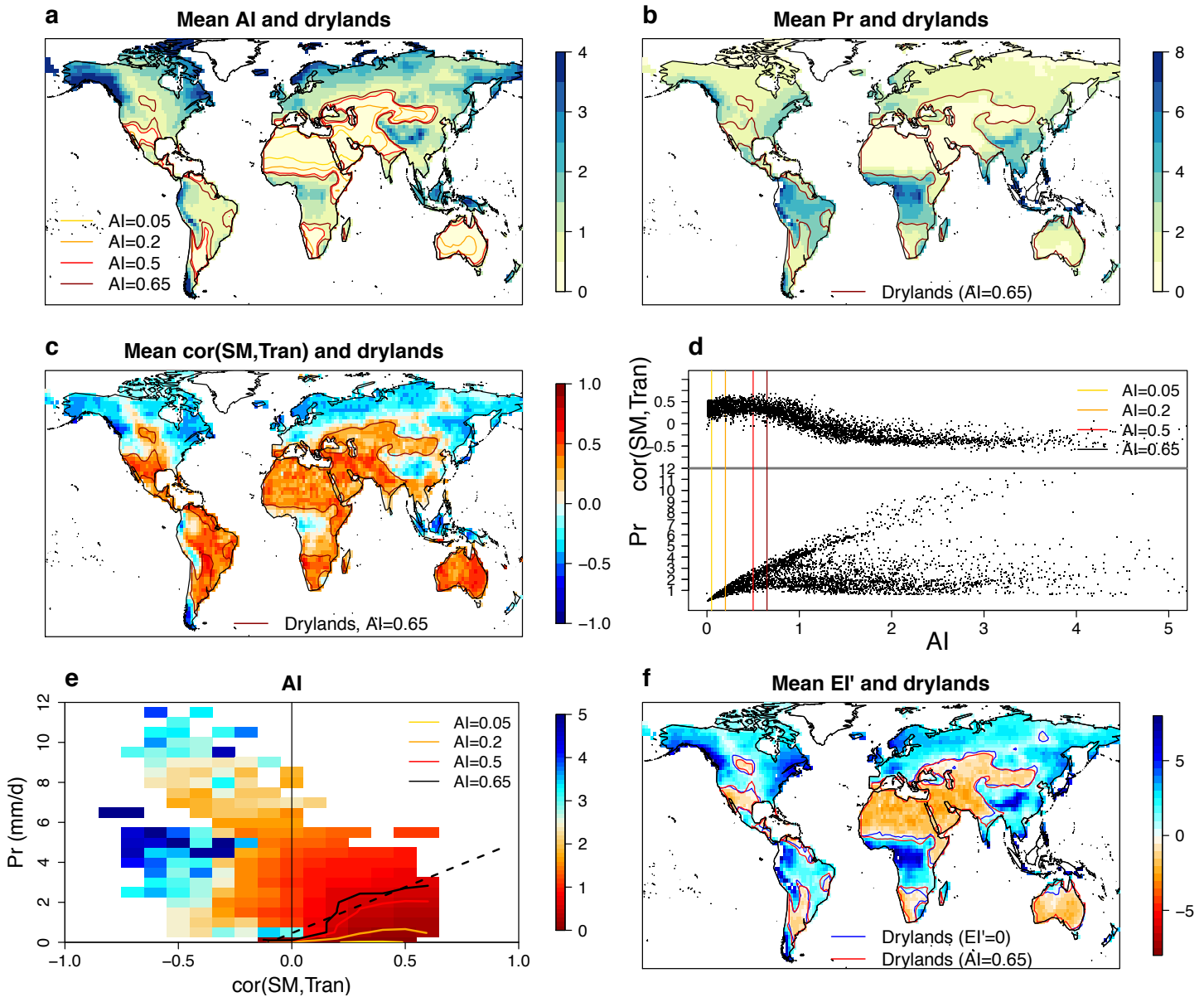

Figure S12: Same as Figure 1, but for EI', an index similar to EI but that includes mean annual precipitation instead of mean annual LAI. (a) Multi-model mean Aridity Index (AI) in 12 CMIP5 models (Methods; Table S1) and corresponding drylands classification over 1971-2000 (see caption of Fig. 1); (b) Multi-model mean annual precipitation (Pr; mm/d); contour line represent drylands according to the AI-based definition (AI<0.65); (c) Multi-model mean temporal correlation between annual-mean top-10 cm soil moisture and transpiration; contour line as in (b); (d) Relationship over

*global land between AI and Pr (mm/d) and cor(SM,Tran), from (a), (b) and (c), with vertical lines corresponding to AI thresholds denoted in (a); (e) Multi-model mean AI binned as a function of mean cor(SM,Tran) and mean Pr; the dotted line is an optimal linear fit to the contour line for AI=0.65 (in black); as for the initial EI, the coefficients from that linear regression are used to define EI', which then yields: EI' = Pr – (a*cor(SM,Tran)+b) with a=4.6 and b=0.46; (e) Multi-model mean EI'; contour lines indicate drylands based on the AI and EI'.*

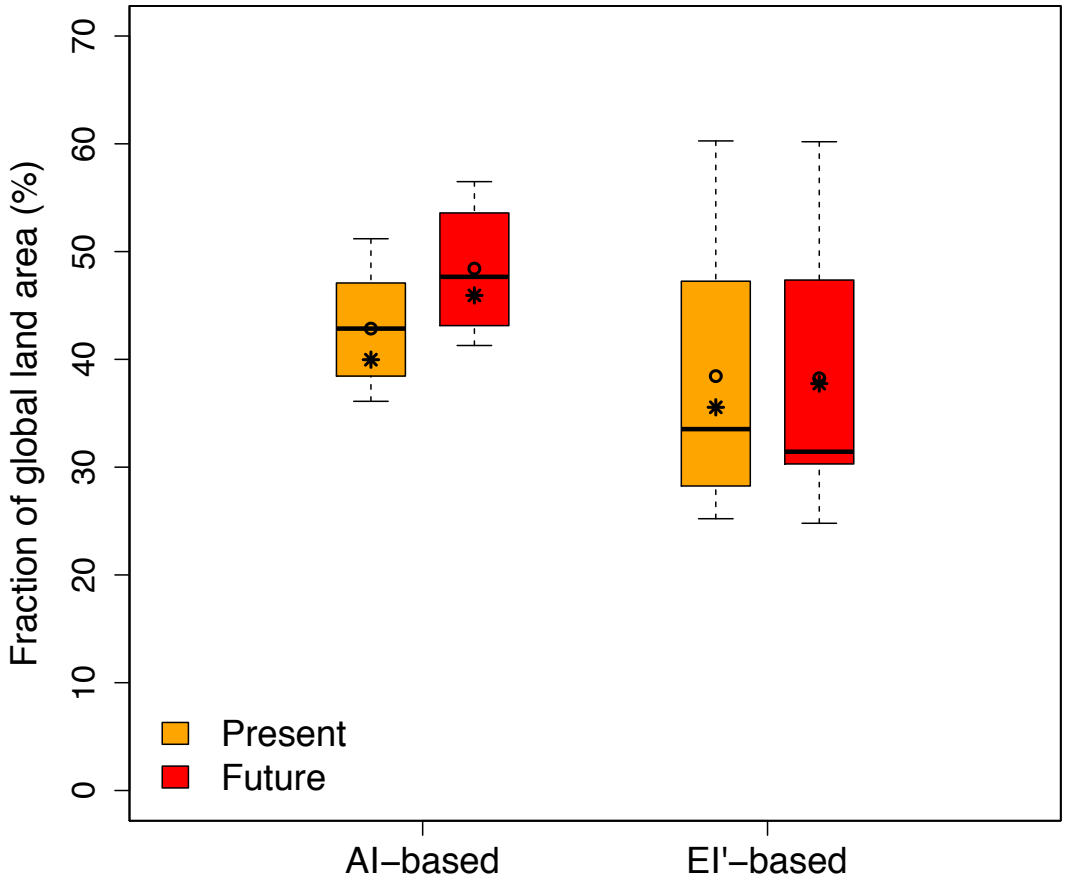

Figure S13: Same as Figure 5 but with EI' instead of EI. Distribution of global fraction of drylands in CMIP5 models in the present (1971-2000) and future (2071-2100, RCP8.5), based either on the AI definition (left) or the EI' definition (right). Box edges represent the first and third quartiles of the CMIP5 distribution, the straight line is the median, the dot is the mean, and whiskers represent the entire range. The star indicates the drylands fraction in the multi-model mean.

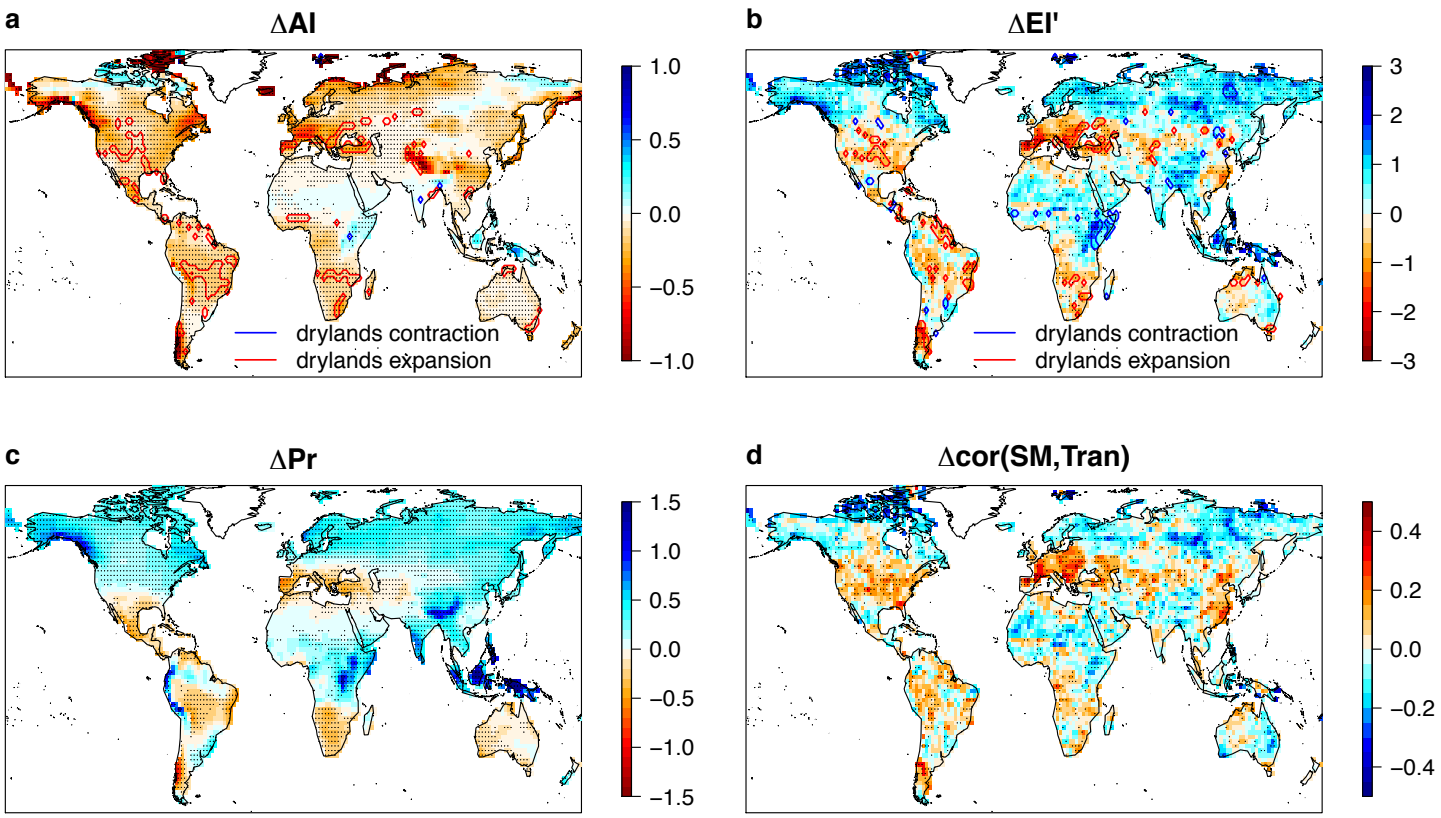

Figure S14: Same as Figure 2, but with Pr and EI' instead of LAI and EI. (a) Mean change in Aridity Index between 1971-2000 and 2071-2100 in RCP8.5 scenario. Contour lines indicate changes in drylands defined based on AI; (b) Same as (a), for EI'; (c) Mean change in annual Pr (mm/d); (d) Change in correlation between annual mean surface soil moisture and transpiration. Stippling indicate where more than three quarters of models agree on the sign of change.

References:

1. Taylor, K. E., Stouffer, R. J., & Meehl, G. A. An overview of CMIP5 and the experiment design. *Bull. Am. Met. Soc*. 93, 485-498 (2012).

2. Milly, P. C. D. & Dunne, K. A. Potential evapotranspiration and continental drying. *Nat. Clim. Change* 6, 946–949 (2016).

3. Yang, Y., Roderick, M. L., Zhang, S., McVicar, T. R. & Donohue, R. J. Hydrologic implications of vegetation response to elevated CO2 in climate projections*. Nat. Clim. Change* 9, 44–48 (2019).

4. Mankin, J. S., R. Seager, J. E. Smerdon, B. I. Cook & Williams, A. P. Mid-latitude freshwater availability reduced by projected vegetation responses to climate change. *Nat. Geosci.* 12, 983-988 (2019).